Predicting phase behavior in high entropy and chemically complex alloys

James R. Morris[1*], M. C. Troparevsky[2], Louis J. Santodonato[3], E. Zarkadoula[4] and Andreas Kulovits[5]

[1]Ames Laboratory, Ames, IA 50011

[2]Oak Ridge National Laboratory, Oak Ridge, TN 37831

[3]Advanced Research Systems, 7476 Industrial Park Way, Macungie, PA 18062

[4]Arconic Inc., Pittsburgh, PA

Abstract

The interest in high entropy alloys and other metallic compounds with four or more elements at near-equiatomic ratios has drawn attention to the ability to rapidly predict phase behavior of these complex materials, particularly where existing thermodynamic data are lacking. This paper discusses aspects of this from the point of view of predicting without utilizing (or fitting) experimental data. Of particular interest are heuristic approaches that provide prediction of single-phase compositions, more rigorous approaches that tackle the thermodynamics from a more fundamental point of view, and simulation approaches that provide further insight into the behaviors. This paper covers cases of all three of these, in order to examine the strengths and weaknesses of each approach, and to indicate directions where these may be utilized and improved upon. Of particular interest is moving beyond "which composition may form a solid solution," to recognizing the importance of underlying thermodynamic realities that affect the temperature- and composition-dependent transformations of these materials.

1. Introduction

In the last 10 years, a huge interest and body of literature emerged on "high entropy alloys," single phase solid-solution alloys with a large number of constituents in nearly equal atomic ratios [1-10]. Such alloys have no well-defined primary element or binary system, making them significantly different from currently used alloys such as steels, Al alloys that are important structural alloys in the automotive and aerospace industry, Ti-, and Ni-based superalloys that are essential for intermediate and high temperature applications, and other alloys that have remarkable properties that can be understood qualitatively based on binary and established relevant sections of ternary phase diagrams. Research in the area of 4 to 5 near equiatomic element systems has shown that at least some of these alloys exhibit remarkable properties. For example, face centered cubic (FCC) systems show significant strength and ductility [5], leading to a very high toughness. The true, enormous potential that these systems offer theoretically, is the possibility of intrinsic materials property optimization through chemistry control.

The vast number of possible combinations, too large to explore experimentally in the absence of a rigorous, predictive, robust thermodynamic theory for concentrated solid solutions, created a strong interest in predicting and understanding which compositions may form single phases, from the outset. The predictions tend to fall into three separate approaches: physics-based phenomenological models, first-principles techniques that utilize non-empirical approaches to understand properties, and thermodynamic database approaches that rely upon thermodynamic models based primarily on experimentally observed information related to phase diagrams.

The present paper reviews approaches that utilize first-principles approaches, primarily for understanding the prediction of single-phase solid-solution alloys, but also for understanding important microstructure

[*] Contributing author: morrisj@ameslab.gov

formation in related alloys, and the underlying thermodynamics. The review does not delve into the first-principles calculations themselves, but rather on approaches that rely upon these. There are continued challenges with such predictions, particularly evaluating any given approach. The review particularly focuses on our own approach [11, 12] which was motivated by experimental work [4] that provided an ideal test for such predictions. Our approach, described below, was essentially based on a phenomenological assumption: if any two types of atoms *either* strongly preferred to segregate from each other, *or* strongly preferred to form ordered phases, then the alloy would tend to form multiple phases.

Since that publication, there have been both new approaches, and a very large number of new experimental results. The purpose of this paper is to examine our original model, in light of these results, particularly considering both the potential applications of the model beyond its original intent, but also to consider critically its assumptions, and to compare with new approaches (particularly the approach of Ref. [13]. Ultimately, the approach has been useful, but it is based on some empirical assumptions, rather than more rigorous thermodynamics. Moreover, it does not fully consider the thermal history of the material and how that may (or may not) allow for the formation of a single-phase. The latter is important, as it is now apparent that many observed single phase alloys are metastable, formed by cooling from higher temperatures where the single phase may be thermodynamically stable. For example, the Cantor alloy, CoCrFeMnNi, has been the "model" HEA, but has been shown to decompose in appropriate annealing conditions [14, 15]. While a full kinetic assessment is not reasonably achievable from first-principles calculations, there are arguments that may be considered, and we discuss these below.

The paper is organized as follows: In section 2, we discuss the prediction of single-phase solid solutions, particularly in comparison with experimental results summarized in the work of Gao et al. [1]. We particularly pay attention to alloys with Al as a constituent. Al is commonly used in chemically-complex alloys (which we use to denote multicomponent alloys with nearly equal constituents, whether or not they form single phase). Moreover, we demonstrate that this forms a challenge to our approach of [11, 12], and discuss the underlying reason for this. We further compare with an alternate approach of Lederer et al. [13] (which we refer to as the LTVC approach, denoting the authors of that paper) that considers the statistical mechanics of the systems, and that suggests a very reasonable criterion for single-phase formers, that the alloy be thermodynamically stable at some temperature below melting, thus permitting a single phase to be formed in equilibrium, and potentially cooled in a way that retains the single phase (perhaps in a metastable state). In section 3, we examine the use of our enthalpy matrix to understanding phase evolution more directly. We review the recent work [16] examining phase evolution in a series of $Al_xCoCrFeNi$ alloys, where Monte Carlo simulations based on the enthalpy matrix produces results remarkably similar to experimental observations, and present new work applying the approach to a reported single-phase solid solution $Al_{20}Li_{20}Mg_{10}Sc_{20}Ti_{30}$ [17]. This composition violates the criteria described in [12], both because of pairs of elements such as Ti-Al that are intermetallic formers, and because of pairs such as Li-Ti that as binaries do not have any mutual solubility. Despite this, we provide Monte Carlo results that support the possibility of forming a single phase in this system. We close section 3 with a broader discussion of Monte Carlo simulations and related approaches.

2. Predicting single-phase solid solutions

The challenge of predicting single-phase solid solutions, particularly from a "first-principles" approach, is due to the sheer combinatorial challenge of considering competing phases for a given compound, when there are 4 or more elements at significant concentrations. This is easily demonstrated by considering a particular 4-component BCC HEA, AlNbTiV [18]. The phase stability of this is determined not only by the Gibbs free energy of the BCC phase, but also by the competing free energies associated with *all possible transformations*. Thus, in principle, this is a huge search space and associated minimization

problem, even with the assumption that the Gibbs free energy is readily available. To determine the Gibbs free energy of the BCC solid solution (and of the competing phases), one properly needs to make simplifying assumptions, such as assuming an ideal entropy of mixing, and that the enthalpy may be calculated using a quasirandom structure [19]. Such treatments of short-range order, however, come with their own simplifying assumptions. The presence of Al, and its strong interactions with the other elements, suggests that short-range order cannot be ignored, rendering random or quasi-random mixing assumptions suspect. The degree of short-range order, which is also a function of temperature, has been challenging to treat rigorously. Alternately, one may explicitly model the short-range order using techniques such as Monte Carlo simulations (as demonstrated in Section 3 below). (Although not a focus of this work, recent linear response approaches [20] provide ways of not only considering short range order, but also their relationship to ordered phases.) We also note that other contributions to the enthalpy and entropy should properly be accounted for. This includes the role of vibrational entropy [21-27] in stabilizing particular phases, as well as a proper evaluation of the configurational entropy (beyond the "ideal" estimate) that accounts for the short-range order in disordered and weakly ordered alloys (such as Al-containing alloys discussed below).

In this section, we discuss two very different approaches for predicting single-phase solid solutions. Section 2.1 describes our own heuristic approach [11, 12] that has been reasonably successful, based upon a simple approach based on an enthalpy matrix derived from first-principles databases. Since its original publication, there have been a large number of new experimental results, and we use these to test the original approach. For alloys without Al, the approach is shown to be robust, in comparison with results collected by [1]. However, Al-containing single phases, such as AlNbTiV, clearly fail this approach. We discuss the issues with Al in section 2.2 below. A very different approach by Lederer et al. [13] attempts a more proper treatment, estimating the minimum temperature at which a given composition will form a solid solution (including the prediction that the AlNbTiV and AlCrMoTiW compounds form a solid solution). Section 2.3 below describes comparisons of the results of these methods, revealing differences, strengths and weaknesses of each.

2.1. Testing the "minimum/maximum" enthalpy approach for alloys without Al

As with all novel alloys, the challenge is not only to understand what phases are likely to be present at a given temperature and composition, but to provide some insight into the observed behaviors. The observation of single-phase solid solutions with 5 or more equiatomic components emphasizes the importance of configurational entropy (often approximated by the ideal entropy of mixing, though the actual entropy undoubtedly deviates from this). This clearly plays an important, but incomplete role: certainly, not all five-element metallic equiatomic alloys can be formed into a single-phase structure. As an important demonstration of the limit of a simple entropic argument, Otto et al. [4] examined variations of the "Cantor" alloy CoCrFeMnNi [3], substituting one of the elements with another with similar properties such as crystal structure and size. For example, replacing Ni with Cu results in a multiphase alloy, even though Ni and Cu form a very good solid solution, have similar electronegativities, and similar sizes. In fact, in the work of [4], all such substitutions tried resulted in multiphase compounds.

This has led to a number of heuristics attempting to understand and predict which alloys may form single phases. A simple and intuitive example is to examine the average enthalpy of mixing and size variation of the elements. Alloys with strongly negative average enthalpies and/or with strong size variations are unlikely to form single-phase solid solution alloys. However, this is not strongly predictive: for example, a comparison of the Cantor alloy with the alloy formed by substituting Cu for Ni produces an alloy with a very similar measure of size variation, and an average enthalpy of mixing that is even closer to zero, so this would incorrectly suggest that the Cu-containing compound would be single phase. Recently, Gao et

al. [1] reviewed the literature, tabulating a large set of alloys with experimental observations of whether or not they were single phase. They also compared a number of heuristic approaches against these observations, and none were strongly predictive.

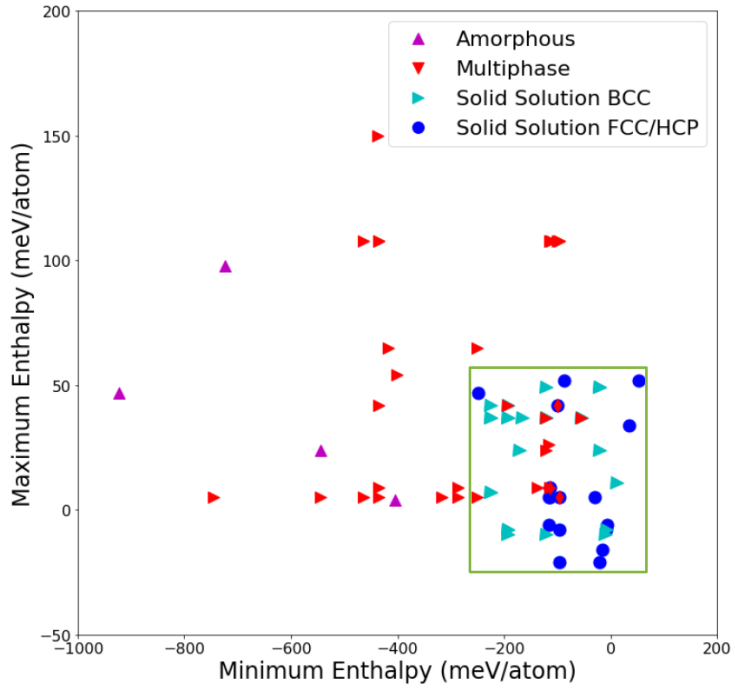

Figure 1. Examination of alloys from Ref. [1] in terms of the highest and lowest enthalpies of pairs of atoms, taken from Table 4. Only alloys without Al are shown. Alloys that form single phase solid solutions are clustered in the bottom right. The green box shows the regime where most single-phase solid solutions are found.

In 2015, Troparevsky et al. [11, 12] proposed a heuristic based solely upon first-principles calculations of the formation enthalpies of the binary components. The fundamental insight behind this approach is that if two elements have a strong driving force to form a compound, or to phase-separate, then forming a single-phase solid-solution will be challenging, independent of the "average" enthalpy. From this hypothesis, one should examine all pairs of mixing enthalpies in the compound, and to form a single phase, one should choose alloys where no pair has a strong driving force for intermetallic formation, and where no pair has a strong driving force for phase separation. Thus, instead of examining the *average* enthalpy of mixing, this approach examined the *extreme values* of the set of enthalpies. This had a number of successes, including that it correctly predicted that of the alloys examined by Otto et al. [4], only the Cantor alloy would be single phase. We note (and discuss further in the Discussion section) that the approach does not make any significant estimate of the entropy, particularly any estimate that is dependent on composition or that deviates from ideal entropy.

To re-examine this model, we consider the alloys tabulated in Ref. [1] and their outcome. We note that this approach does not consider the actual composition of the alloy, considering only the elements forming the material. This is obviously an oversimplification, but for now, we do not move beyond this. For each alloy in that work, we calculated all pairs of enthalpy, using Table 4 (Appendix 1) which is an updated version of that presented in [12]. This table is derived from high throughput calculations, particularly those from the AFLOW database [28] and from those of Widom [29]. In Table 4**,** the values represent the *smallest enthalpy compound found from high-throughput calculations across a wide number of crystal structures.* (Table 4 has some updates from Ref. [12] due to changes in these datasets, as discussed in Appendix 1.)

We separate the alloys from [1] into four sets based upon their tables: (1) alloys that form close-packed [face-centered cubic (FCC) or hexagonal close packed (HCP)] single phases; (2) alloys that form single phase body-centered cubic (bcc) solid solutions; (3) alloys that formed multiple crystalline phases; and (4) alloys that form amorphous phases. There are issues specific to some elements, most notably Al, which

we focus on in later sections. For those alloys without Al, we have plotted each of the four sets in Figure 1, as a function of their highest and lowest enthalpies of mixing calculated from Table XXX. This clearly results in a close-clustering of the sets of single phase solid solutions in the bottom right of the figure: all single phase alloys have a maximum enthalpy of mixing below 55 meV/atom, and a smallest enthalpy of mixing greater than -250 meV/atom. We also see that the bcc single-phase solutions appear to occur more often at lower minimum enthalpies than those of the FCC solid solutions. This is consistent with the observation [12] that the lowest value used in the criterion appears to be correlated with the annealing temperature, and that the refractory bcc-based systems tend to have higher melting (solidus) temperatures, and therefore may be quenched from a higher temperature. As in Ref. [12], we note that this approach correctly predicts that none of the Cu-containing alloys listed in [1] form a single phase, due to its strong tendency to phase separate with most metallic elements (particularly Cr and Fe).

Moreover, within the regime where most of the single phase alloys are found (minimum enthalpy > -200 meV/atom, maximum enthalpy < 55 meV/atom), there are relatively few multi-phase alloys. This suggests that this approach generates few false positives. A closer view of these cases, where the model appears to predict single phase but the data from [1] indicates otherwise, provides more insight: first, several of these compounds include Cr-Ti, which we have already noted is problematic from a first-principles point of view, associated with the formation of a Cr_2Ti Laves phase. Similarly, one "false prediction" for NbTiVZr. Examining this more closely, one sees that the V-Zr phase diagram has a Laves phase V_2Zr Laves phase that is stable to 1300 °C. The stability of this intermetallic phase strongly suggests a large magnitude, negative enthalpy of mixing, whereas the present AFLOW data shows only positive enthalpies of mixing for V-Zr compounds. Thus, for alloys with combinations of Cr-Ti or V-Zr, the issue may not be the model, but instead the data that feeds into the enthalpy matrix used by the model.

The remaining red data points in this regime actually correspond to single phase formers, including the Cantor alloy CoCrFeMnNi – the classic example of an FCC single phase. The two others correspond to related four component alloys that have been observed as single phases, CoCrFeNi and CoCrMnNi. This reflects the fact that at room temperature, many of the observed single-phase materials are metastable: they are not thermodynamically stable. Thus, whether or not they are single phase does not have a unique answer: some alloys may be able to form into a single phase *or* multiple phases, depending upon the thermal history of the material. So again, the issue may not be the model, but rather the common fact that the materials formed may depend on the history of the material.

This demonstrates that this approach is reasonably successful, *for those alloys without Al.* Overall, the method successfully clusters the single phase formers, while excluding the alloys that are not known to form single phases. Exceptions appear to be due to questions of the completeness of the enthalpy matrix, or due to the fact that many single-phase formers may *also* be observed as multiphase. Of course, this highlights the question we address below: what is different about Al?

2.2. Testing the "minimum/maximum" enthalpy approach for alloys with Al

In the previous section, we examined alloys without Al. We now turn our attention to those with Al, and discuss in (slightly) more detail why this approach presently fails for this. We note that amongst the single-phase, solid-solution compounds identified in [1], there are a number of Al-containing single phases. These are listed in Table 1, along with their crystal structure, the minimum and maximum enthalpies from the enthalpy matrix, and the pairs of elements that correspond to the enthalpies. We immediately see that the minimum enthalpies range from -428 meV/atom to -677 meV/atom. This clearly violates the condition listed above, H_{min} > -250 meV/atom. This is not surprising, as Al is a strong

intermetallic former, particularly for elements like Ni, Ti and Zr; yet, Table 1 has entries containing all of these. Why is it that despite this, one may form solid solutions with Al combined with these elements?

The answer to this comes from the realization that H_{min} does *not* necessarily represent the enthalpy drop that occurs as one changes from a solid solution to an ordered phase. If it were the case, then a crude estimate of the ordering temperature could be taken by setting the free energy of the solid solution to $-TS_{config}$ (neglecting the enthalpy of the solid solution), and the free energy of the ordered phase to H_{min} (neglecting configurational and other contributions to the entropy). A further simplification may be made by assuming S_{config} may be represented by an *ideal* solution.

If, however, the enthalpy of the solid solution is a significant fraction of H_{min}, then the crude estimate must account for this. In fact, Al will form a low enthalpy solid solution with a number of elements at high temperatures. The simplest example is for Ti-Al, which has a large negative enthalpy of mixing, yet Al has significant solubility in both HCP α – and BCC β-Ti for temperatures above the α – Ti solvus. For instance, the maximum solubility of Al in a – Ti is ~ 22 at.% at 1373K and ~ 44 at.% at ~1740 K. Yet the enthalpy matrix approach for predicting single phases – without accounting for the solid solution enthalpy – fails to capture this.

One can make a crude estimate under the assumption that the contributions to the enthalpy are pairwise. As an example, consider the $Ti_{0.75}Al_{0.25}$ composition (atomic fractions) in the solid-solution α-Ti phase. In an *ideal* solution, each Al atom will have (on average) 75% of its near neighbors being Ti, and 25% Al atoms. The large number of favorable Ti-Al neighbors give a low enthalpy associated with this solid solution. In the completely ordered phase, Al will have *only* Ti neighbors. Thus, the number of Al-Ti near neighbors will increase by only one third – and thus, in a simple near-neighbor model that ascribes H_{min} to the number of favorable Ti-Al neighbors, the enthalpy *change* from a random solution to a highly ordered system will only be ¼ H_{min}. In fact, short-range order in the solid solution will likely *increase* the number of favorable nearest neighbors, reducing this further. Thus, the enthalpic driving force for ordering is significantly reduced. (This type of near-neighbor approach was applied to Monte Carlo simulations of the $Al_xCoCrFeNi$ system with reasonable comparison to experiment [16], as we will discuss in Section 3.)

Thus, properly, the enthalpy matrix should be modified by subtracting out the enthalpy of the solid solution composition. In [12], this was accounted for in the case of Re, using an estimate of the solid solution enthalpies. For cases where there is little mutual solubility, the enthalpy matrix reasonably considers the *separate* phases. But in the case where there is mutual solubility in a disordered phase, then this needs to be modified. This is similar to the Hume-Rothery rules: when different atoms may coexist on a similar lattice, with a similar lattice parameter, then one must consider the possibility of forming a solid solution, to determine the thermodynamic behavior.

Table 1. Al-containing solid solutions, from Ref. [1], along with their minimum- and maximum-enthalpy pairs from the enthalpy matrix.

Compound	*Structure*	H_{min} (meV/atom)	*Lowest pair*	H_{max} (meV/atom)	*Highest pair*
$Al_xCoCrFeNi$ *x=0.25, 0.3, 0.375*	FCC	-677	Al-Ni	5	Co-Cr
AlNbTiV	BCC	-428	Al-Ti	37	Ti-V
AlCrMoTiW	BCC	-428	Al-Ti	42	Cr-Mo
$AlCr_{0.5}NbTiV$	BCC	-428	Al-Ti	37	Ti-V
AlNbTiV	BCC	-428	Al-Ti	37	Ti-V

$AlNb_{1.5}Ta_{0.5}Ti_{1.5}Zr_{0.5}$ $Al_{0.3}NbTa_{0.8}Ti_{1.4}Zr_{1.3}$	BCC	-539	Al-Zr	36	Ta-Zr
$Al_{0.4}Hf_{0.6}NbTaTiZr$ $Al_{0.75}HfNbTaTiZr$	BCC	-539	Al-Zr	49	Hf-Ta
$Al_{0.3}NbTa_{0.8}Ti_{1.4}V_{0.2}Zr_{1.3}$	BCC	-539	Al-Zr	37	Ti-V

2.3. Incorporating statistical mechanical treatments

The sections above show that, phenomenologically, a min/max enthalpy approach appears to be successful for alloys that do not contain Al, and indicates some of the difficulties both for Al-containing alloys, and more broadly. Furthermore, despite the interest in high entropy alloys, the discussion of the role of temperature and entropy are largely left implicit in the heuristic approach. The enthalpy window described in section 2.1 in fact has no reference to composition, temperature, or entropy. In [12] the value of H_{min} was rationalized in terms of the annealing temperature and the (ideal) entropy of mixing, much like the simple argument presented in Section 2.2 for an ordering temperature. The case of Al indicates that a more systematic approach would be useful, that properly considers potential phase transformations, both ordering and phase separation, and that accounts for both the enthalpies and entropies that contribute to both the ordered and disordered phases.

The approach also does not truly address the issue of metastability: for a given alloy, the phases present may not represent true thermodynamic equilibrium, and therefore may be a function of the history of the alloy. A high temperature solid-solution may potentially be quenched to room temperature. The heuristic approach may make simple arguments, but the question "Can a given composition be formed into a solid solution" really is not well phrased, as it depends upon the processing history of the material.

Lederer *et al.* [13] (termed "LTVC" in that paper and below) pose a better phrased problem: is there a temperature, below the melting temperature T_m, where there is a thermodynamically stable, single-phase, solid solution? This is better phrased, as it asks a thermodynamic question that can (in principle) be attacked rigorously. Moreover, this is quite physical: if there is a temperature where the solid solution is thermodynamically stable, then in principle, the system could be quenched to produce a metastable single phase at lower temperatures. Similarly, Santodonato et al. used Monte Carlo simulations to examine the single phase stability of $Al_xCoCrFeNi$ (further discussed below), and compared the ordering temperatures to the melting temperature [16]. Lederer et al. [13] used a common approach to estimate the melting temperature (by averaging the melting temperatures of the elements), and a statistical mechanical approach to estimate a temperature T_c above which the alloy will be single phase. The LTVC approach estimates an order-disorder temperature T_c by examining the possible energetics of an n-site cell (with n chosen to be 8, though they also test $n=12$ for comparison, depending upon its composition and configuration, based upon a cluster expansion [30-33] fitted to data from the AFLOW database [28] using the ATAT software package [34]. They then use a mean-field approach, the generalized quasichemical approximation (GQCA) [35, 36] to estimate a temperature-dependent population of the cell. By defining an order parameter in terms of the population of an equiatomic cell and its overlap with a random population (the high temperature limit), they calculate T_c for the equiatomic composition by examining where the order parameter changes most rapidly. From that, they further extrapolate the order-disorder transition across compositions. This is done for both BCC and FCC lattices, with the phase chosen to minimize the thermodynamic potential. They also incorporate potential ordered phases through the use of the AFLOW database. LTVC further compare with an estimate $\tilde{T}_c$ that is constructed through comparison of the thermodynamic potential of a high-temperature limit with the AFLOW convex hull.

Another approach, that has similarities to both [12] and LTVC, is provided in King et al. [37]. Their approach uses an ideal entropy of mixing and a Miedema estimate for enthalpies (see [38]), to estimate both the free energy of formation of the solid solution phase, and the free energies of forming potential competing binaries (either through phase separation or ordering) from the solid solution. This allows for an estimation of the lowest temperature where the solid solution is stable. By comparing this temperature to an estimated melting temperature, as in LTVC, they can examine the composition-dependent possibility of forming a solid solution at some temperature below T_m. As in [12], the approach examines the most strongly competing binary phase, which is largely determined by the change in the enthalpy associated with this competing binary. Though the approaches [12] and [37] for estimating these enthalpy changes are quite different, the spirit is similar.

2.3.1. *Comparison of the enthalpy approach with results from LTVC.*

As indicated above, the LTVC criterion, that a transition occurs at T_c below the melting temperature T_m, is that $T_c/T_m < 1$. From this, they predict a series of 4 and 5 component solid solution alloys that have been observed (see Table 2 from that paper). Interestingly, the experimentally listed ones shown in their Table 2 also fall within the enthalpy "window" in Figure 1, except for the two Al-containing compounds AlNbTiV and AlCrMoTiW. As above, the min/max enthalpy approach appears to work for those alloys without Al.

We now compare some predictions of LTVC [13] and of [12] for those that do not contain Al. For specificity, we restrict ourselves to the case of the quaternaries listed in Table 5 of [13]. We re-frame the enthalpy criteria by scaling the minimum and maximum pairs by k_BT_m utilizing the same values for T_m given in Table 5 of [13]. For each alloy, we calculate the lowest and highest enthalpy pairs, and scale them by k_BT_m. The single phase formers identified in Ref. [1] are found to satisfy the dimensionless criteria:

$$H_{min}/k_BT_m > -1.0 \; ; \; H_{max}/k_BT_m < 0.3 \qquad (1)$$

Of the 460 quaternaries without Al that the LTVC approach predicts to be single-phase solid solution using, 179 also satisfy the criteria in Eq. (1). Thus, while there are significant overlaps, most of the predictions differ. There are important sets of differences, as discussed below.

2.3.2. *Cases which violate the maximum enthalpy condition, $H_{max}/k_BT_m>0.3$:*

Of the quaternaries where the LTVC approach predicts a single phase, 158 compounds have a higher "maximum" enthalpy of mixing than the above criterion. These compounds are listed in Appendix 2. Thus, for these compounds, LTVC predicts a single phase, while the min/max criteria suggests phase separation. The cases where these predictions disagree are dominated by alloys containing the noble metals Au, Ag and Cu. In [12], it was already noted that equiatomic alloys with Cu are unlikely to form single phases. Indeed, the compilation of [1] show no ternary or higher-order solid solution phase containing Au, Ag or Cu. In contrast, the LTVC approach indicates that there should be a large number of such phases. For example, LTVC predicts that the AgAuPdRu should have $T_c=280$ K, despite the fact that Ru is essentially immiscible with Ag, Au, and Pd at temperatures below 800 K. Thus, it may be a challenge to form HEAs containing "noble" metals. Other than those containing Au, Ag or Cu, the quaternaries that LTVC predict to be single phase but violate $H_{max}/k_BT_m < 0.3$ contain Pd-Os, Pd-Ru, or both.

What are the limits of this? Recently, Gao et al. [39] reported a new filler metal $Fe_5Co_{20}Ni_{20}Mn_{35}Cu_{20}$ that formed a Cu-Ni-Mn phase. Could a solid solution form for equiatomic CuMnNi? The LTVC paper predicts that it will not (see Table 4 of [13]). In contrast, the min/max approach indicates that it should be able to. It is not surprising that Cu and Ni mix easily; however, at high temperatures, Cu-Mn and Mn-Ni both form FCC phases with wide solubilities. Thus, we suggest that this is a likely single-phase former, at least when quenched from elevated temperatures.

2.3.3. *Cases which violate the minimum enthalpy condition, $H_{min}/k_BT_m<-1.0$:*

Of the 486 quaternaries that LTVC predict to form solid solutions below T_m, we identify 160 that have $H_{min}/k_BT_m<-1.0$, which could suggest that these are likely to form ordered phases. As we discuss below, the interpretation is more subtle.

The most extreme cases have $H_{min}/k_BT_m<-3.0$, and are summarized in Table 2. These are dominated by the chemically similar Nb-Ir, Nb-Pt and Nb-Rh interactions. All three of these are predicted by LTVC to have $T_c/T_m<0.5$, which would indicate that they would form solid solutions at relatively low temperatures (relative to melting). In contrast, the enthalpy matrix approach would suggest these would be strong intermetallic formers. Interestingly, LTVC makes a secondary approximate estimate for T_c (using their Eq. 8, indicated as $\widetilde{T_c}$ in their paper and in Table 2 below). For these compositions, this "approximated" $\widetilde{T_c}$ is much higher than their values of T_c, higher than the melting temperature. Thus, if one uses LTVC's $\widetilde{T_c}$ in place of T_c, then LTVC would also predict no solid solution below melting.

Beyond these extreme cases, one frequent feature of the quaternaries that LTVC predicts to form solid solutions but that violate $H_{min}/k_BT_m<-1.0$ is the presence of Re. 70 of these are ruled out due to low enthalpy pairs with Re. Of these, 25 compounds have the lowest enthalpy pair corresponding to Pt-Re (with a value of -232 meV/atom). One might expect then that Pt-Re would form an intermetallic. However, the phase diagram is dominated by a Pt-rich FCC solid solution, and a Re-rich HCP solid solution. In our original paper [12], we noted that Re forms a number of low enthalpy solid solutions. Thus, as in some cases of Al, Re can sometimes form low enthalpy solid solutions with little driving force for ordering (as in Pt-Re, as well as Ir-Re and Nb-Re, other cases where the enthalpy of mixing is low). Similarly, a significant number of cases where LTVC predict the formation of solid solution FCC phases involve both Mo and Pt. Mo and Pt have a strong, negative heat of mixing, but form no line compounds, and at higher temperatures, there is a large solubility of Mo in FCC Pt. Thus, again, the ability to form solid solutions must be accounted for, which is not explicitly considered in the enthalpy matrix approach. Thus, in these cases, LTVC more naturally accounts for the possibility of solid solutions with low formation enthalpies, and that therefore have low driving forces for ordering.

Table 2. Quaternary compounds predicted to form solid solutions below T_m by LTVC with $H_{min}/k_BT_m<-3.0$. The predicted T_c is from calculations from Ref. [13], and the estimated $\widetilde{T_c}$ is from their Eq. 8.

Compound	T_c (K)	$\widetilde{T_c}$ (K)	T_m (K)	T_c/T_m	H_{min}/k_BT_m	*Lowest pair*
IrNbPdRh	260	2920	2370	0.11	-4.1	Ir-Nb
NbPdPtRh	220	2640	2210	0.10	-3.8	Nb-Pt
CuNbPdRh	900	2040	2040	0.44	-3.1	Nb-Rh

3. Utilizing the enthalpy matrix for materials with strongly positive and/or strongly negative enthalpies of mixing.

3.1. Applications to $Al_xCoCrFeNi$

The discussion in Section 2 concerning Al demonstrates a limit of the enthalpy matrix approach: a strongly negative enthalpy of mixing does not necessarily imply a strong tendency for intermetallic formation, *if there is a comparably negative enthalpy of mixing associated with the solid solution*. In that case, the *difference* in enthalpies may be small, implying a weak driving force for ordering. This occurs frequently for both Al and also for Re (as discussed above, and also in Ref. [12]).

However, the enthalpy matrix has been proven to be of use for understanding Al-containing alloys, by incorporating the enthalpy matrix information into Monte Carlo simulations of $Al_xCoCrFeNi$ [16]. This approach assumes that the elements can potentially form a solid solution within a single phase, and that the enthalpies of mixing can be mapped into effective interactions suitable for performing the Monte Carlo simulations. In the case of $Al_xCoCrFeNi$, a small amount of Al can stabilize a BCC solid-solution structure (similar to the fact that small amounts of Al in Fe will prevent the formation of the FCC phase) [40]. At low temperatures, the system forms two phases [41]: a B2 aluminide phase (*CsCl* prototype, primarily Ni-Co-Al) that is ordered on an underlying BCC lattice, and a BCC solid solution (primarily Cr-Fe). The fact that these elements can form a solid solution on a BCC lattice, and the primary competing phases are also based on a BCC lattice, makes this ideal for testing with Monte Carlo simulations. The advantage of Monte Carlo simulations is that they can directly probe both short-range and long-range order, without making assumptions about these.

In [16], we demonstrated this approach for $Al_xCoCrFeNi$, examining the progression from a high temperature solid solution through the formation of the B2 aluminide phase. One obvious question is (again) whether a solid solution may occur below the melting temperature. A conventional lattice Monte Carlo simulation does not allow for probing of melting temperatures; however, the experiments probed the melting temperature of the liquid as well as the crystal structure on solidification for *x=1* and *x=2*. The simulations correctly predict that for *x=1*, the B2 ordering occurs slightly below melting, while for *x=2*, B2 superlattice peaks are seen as soon as the system crystallizes. Furthermore, we demonstrated that, for both systems, the ratio of the superlattice peak to the primary peak has a temperature dependence that closely follows the simulated B2 order parameter, for both compositions.

Moreover, the simulations suggest another sharp change in behavior at lower temperatures, near 600 °C for all compositions. The simulations show a change from a highly disordered B2 structure, to one with a significantly higher order, while forming distinct Cr-Fe-rich solid solution regions. The sharpness is demonstrated using short-range order calculations, as shown for *x=1.3* (corresponding to the Al content in the microscopy experiments) in Figure 2. We define $P_{Cr,j}$ as the fraction of near neighbors of a Cr atom

that are of type *j*. Figure 2a shows that $P_{Cr,j}$ exhibits a sharp change near 600 °C: above this temperature, all transition metals are nearly equally likely to be a near neighbor of Cr, and show a similar temperature dependence. Below this temperature, the different transition metals behave very differently: the fraction of Cr-Cr and Cr-Fe neighbors grow rapidly, while those of Cr-Co and Cr-Ni decrease rapidly. Figure 2b emphasizes this, by showing $P_{Cr,Ni}/P_{Cr,Cr}$ as a function of temperature. This is nearly constant above 600 °C, slightly below 1 (indicating that Cr tends to have slightly fewer Ni neighbors than Cr at these temperatures), but drops significantly below this temperature. Experimentally, at low temperatures, the B2 and BCC phases form a coherent microstructure with laths of the two phases; on heating, near 600 °C, *in situ* microscopy showed this microstructure rapidly evolving, supporting the change in behavior.

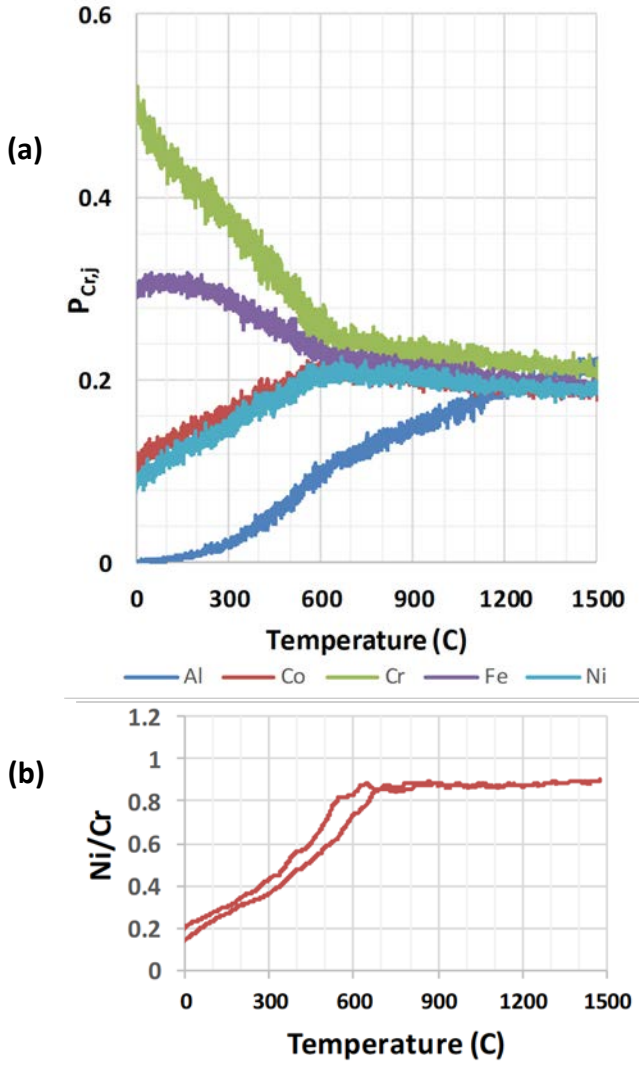

Figure 2. (a) Monte Carlo simulation results for near-neighbor short-range order for Cr atoms, indicating the distribution of atom types of near neighbors of Cr in simulated BCC $Al_{1.3}CoCrFeNi$. (b) Ratio of Cr-Ni and Cr-Cr pairs as a function of temperature. The two curves indicate heating and cooling runs.

3.2. Application to $Al_{20}Li_{20}Mg_{10}Sc_{20}Ti_{30}$

The interest in Al-based materials extends to a variety of alloys. The challenge discussed above shows that the enthalpy matrix approach can be extended, to provide information into complex alloys including HEAs, even when there is a strong interaction that can lead to intermetallic formation (such as Al-Ni and Al-Co). We now ask: is it possible to have a solid solution where there are *both* strong enthalpies of mixing that favor intermetallics, *and* strong enthalpies that favor phase separation? This work is specifically motivated by experimental work showing evidence for a single phase solid solution of the five-component alloy $Al_{20}Li_{20}Mg_{10}Sc_{20}Ti_{30}$ [17]. The reported compound is of interest due to its light weight and reported high strength. This is interesting in several respects: first, in this case, Al strongly interacts with Li, Sc and Ti: Al-Li, Al-Sc and Al-Ti all form intermetallics that are stable up until melting, above the melting temperature of Al. Secondly, Li-Ti and Li-Sc show essentially no mutual solubility in the solid phases at any temperature (and Ti shows little solubility in liquid Li at any temperature below Li's boiling point). Experimentally, casting such alloys is not feasible because the melting point of Ti and Sc are above the boiling point of Li; therefore, Ref. [17] utilized mechanical alloys (ball milling) to generate the materials.

In principle, this is an ideal case for theory: providing potential guidance to alloys where there are experimental challenges to alloy exploration. Furthermore, this material directly challenges the model of Ref. [12], with pairs of elements with strongly negative enthalpies of mixing, and pairs with strongly positive. The values in Table 2 are derived using the AFLOW data [28] and represent the lowest enthalpy of any compound for a particular pair of elements. Table 2 shows the relevant matrix. The strongly favorable Al-Sc and Al-Ti interactions are apparent, as are the strongly repulsive Li-Sc and Li-Ti. Thus, this alloy violates *both* criteria suggested in [12]. However, as discussed above, for Al, strong interactions may not exclude single-phase formation.

	Mg	**Al**	**Sc**	**Ti**	**Li**
Mg	0	-33	2	20	-64
Al	-33	0	-444	-428	-190
Sc	2	-444	0	38	94
Ti	20	-428	38	0	99
Li	-64	-190	94	99	0

Table 3. Enthalpy matrix (see Table 4 in Appendix 1) relevant to the Al-Li-Mg-Sc-Ti alloy, derived from the AFLOW database [28]. All energies in meV/atom.

We simulated this alloy utilizing Monte Carlo as in [16], deriving near-neighbor interactions according to the values given in Table 2. The lattice was chosen to be FCC, due to the observation in [17] that this alloy forms close-packed phases (both FCC and hexagonal close packed [hcp] were reported, depending on thermal history). The simulations show a disordered phase above 700 K. This can be seen both by the snapshot at 700 K shown in Figure 3, but also by the measures of Al-based short-range order on the right side of that figure. This shows specifically the fractions of Ti, Sc and Li amongst the near neighbors of the Al atoms. In a completely random alloy, these fractions would be identical to the atomic composition. Above 650 K, these fractions are indeed close to the alloy composition, and the temperature dependence is weak. One sees that the Ti fraction is closer to 35%, compared to the 30% expected, and similarly the Sc fraction is somewhat higher. This is not surprising, given the strong Al-Ti and Al-Sc interaction. The observation of the disordered phase at higher temperatures supports the observations from [17] that this alloy can form a high entropy solid solution, despite the strong interactions.

As the system is cooled below ~700 K, there is significant ordering. This is indicated both by the sudden changes in the short range order, and by the estimate of heat capacity (determined by energy fluctuations during constant-temperature Monte Carlo simulations). Ultimately, three ordered phases form at low temperatures: Al_3Sc, Al_3Ti, and LiMg (see Figure 3). These low-temperature phases should not be seen as predictive of particular crystal structures, due to the limitation that the simulations were limited to an FCC lattice. Energetically, the observed structures represent plausible sets of compounds that should compete for the low-temperature phase separation, but the particular structures and compositions may not be fully representative. The 100 K structure shown in the figure still shows significant disorder. We attribute this in part due to the use of a nearest-neighbor only model. Preliminary results utilizing a second-nearest neighbor interaction (that preserves the low-temperature energetics of the binary phases) significantly reduces this disorder, while shifting the transition temperature to a slightly higher temperature. The issue of neighbor range is discussed below.

We note that at low temperatures, equilibration is typically expected to become quite slow, due to inefficient exploration of the phase space as characteristic energies become large compared to k_BT. Therefore, the 100 K results shown in Fig. 3 may not reflect true equilibrium. However, we note several

reasons why we believe this is not a serious issue. First, the exchange mechanism for our Monte Carlo simulations that allow for long-distance hopping: pairs of atoms are selected at random, irregardless of distance, for attempted swaps. Thus, atoms several lattice spacings apart are as likely to be swapped as near neighbors. This approach is physically unreasonable, but allows for much faster equilibration as it allows for extremely fast diffusion at all temperatures. We also note that while real diffusive processes depend on activation barriers, the Monte Carlo simulations only consider starting and final configurations, eliminating the role of the energy barrier for atom exchange. Further, Monte Carlo simulations were run multiple times, with similar compositions. In all cases, the results were consistent, suggesting that the system is not "trapped" into a particular configuration. If we assume that, despite this evidence, that the system becomes trapped, then the phases observed in Fig. 3 at low temperatures are indicative of transitions at higher temperatures – which is still consistent with our interpretations of a phase transition near 600 K.

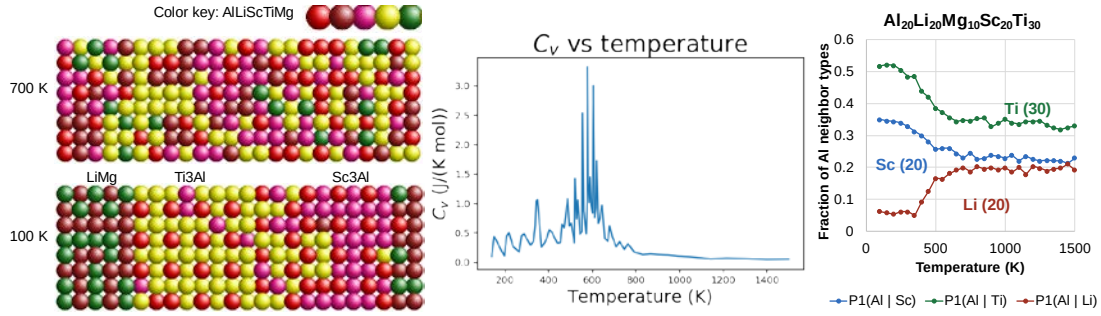

Figure 3. (Left) Monte Carlo results for structures of $Al_{20}Li_{20}Mg_{10}Sc_{20}Ti_{30}$ at 700 K and 100 K, choosing the composition from [17]. (Middle) MC simulated heat capacity vs. temperature for this composition. Results show the possibility of forming a single-phase solid solution above ~650 K, qualitatively in agreement with experimental observations [17]. (Right) Al-based short-range chemical order, based upon the MC calculations.

3.3. Outlook on Monte Carlo simulations and other approaches.

The Monte Carlo results suggest that, by properly capturing the energetics of the lowest energy binary phases (through the choice of parameters based on the enthalpy matrix), that the Monte Carlo approach can capture certain information about finite-temperature behavior. This is clearly limited, by a number of issues: For example, in the present framework, the simulations are based on a single lattice structure. In the experimental results of [41], the composition $Al_{1.3}CoCuCrNiFe$ shows the Cu phase separating out, forming a FCC phase separate from the BCC/B2 based microstructure. Simulating this properly would be much more complex than the work discussed above. Furthermore, the issues of 3-body and longer-range interactions requires

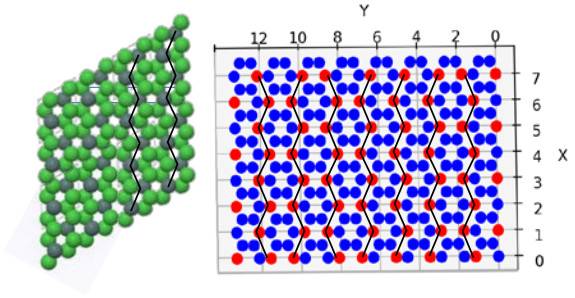

Figure 4. (Left) Ideal low temperature structure of $AlTi_3$. Note alternating "zig-zag" pattern of Al atoms. (Right) Simulated Monte Carlo structure with only near-neighbor interactions. The "zig-zag" structure is not ordered, due to the lack of longer-range interactions.

consideration. For example, if one considers only near-neighbor interactions, some phases may not correctly order. An example is shown in Figure 4, where we performed simulations of ordering of Ti_3Al from a solid solution on an HCP lattice, using our approach above. The known low-temperature crystal structure is shown at left: the Al atoms form a hexagonal pattern. In the figure, the Al atoms can be seen as forming vertical "zig-zag" chains that define the hexagons. On right is the simulated structure. The Al forms similar chains; however, these chains do not alternate as in the original structure, but are randomly organized. This is directly connected to the use of a nearest-neighbor model: in such a model, the disordered structure has an identical energy to the ordered structure, as it preserves the near-neighbor configurations.

However, the approach directly provides information on short range order, and on potential competing phases. The simple demonstrations presented here certainly can be improved upon, yet provides evidence that the approach is promising. There are significant caveats: in the above examples, there are experimental reasons to presume that all of the constituents at least have the potential of forming a solid-solution phase that is at least competitive with other possibilities at elevated temperatures. In cases where there are ordered phases that may form, but no lattice structure where a solid solution phase is competitive, then we would not expect Monte Carlo, based upon our enthalpy matrix, to produce reliable results due to the assumption of a fixed lattice. One may envision Monte Carlo approaches that let different lattice structures compete; however, it is not apparent that the simple approach presented here would be reasonable, as it is not clear that a single set of interaction parameters would be applicable in different lattice structures. Moreover, the approach would have to account for the difference in energies between lattices, both for individual constituents as well as the disordered alloy. (In some cases, ordered phases would also need to be accounted for; as an example, at some temperatures there are close competitions between Ti_3Al ordered lattice structures.) The simple selection of parameters, based upon the lowest enthalpy phase as we have done above, does not necessarily reflect the interactions in different lattices. We note that there are great opportunities to improve upon this, by utilizing the much more extensive data available in the binary databases, including enthalpies in a variety of lattice structures. Making use of the fuller data available is both an obvious and attractive approach to deriving more realistic interactions. The successes demonstrated above of our simple approach above should not be considered a generally applicable approach, but rather a first indication that first-principles databases can provide important input to finite-temperature behavior on phase stability in complex alloys.

4. Discussion

This review demonstrates both progress and important issues for *ab initio* based approaches for predicting single phase high entropy alloys, as well as related phase behaviors in near-equiatomic alloys with large numbers of constituents. In general, the development of high throughput databases (such as the AFLOW database [28], which is important for all calculations presented here) in the last 10 years provides very important information, both for prediction of single phases and for our approach to Monte Carlo simulations. Central to our own approach [11, 12] has been is the reduction of the multicomponent nature to a series of pair interactions amongst the constituent species, and the further reduction of this to a simple matrix formed of the lowest formation enthalpies amongst the potential formation enthalpies across many potential compounds for each pair. This series of simplifications is physically motivated, but provides little rigor. It does not account for crystal structure, for actual compositions, or for potential three-element effects. Despite this, the approach provides important predictability. In the present article, we have re-examined the successes and failures of this approach, in light of significantly increased experimental data (as summarized in [1]). As shown in Figure 1, for compounds that do not include Al, the data from [1] indicate that our original approach is quite predictive, identifying a region where nearly all single-phase

formers lie, and that excludes nearly all others. For those containing Al, our approach is much less consistent; we attribute this to the fact that Al will form solid solutions with a low enthalpy of mixing with a number of elements, and therefore has a lower driving force for ordering than our matrix predicts. In our original paper [12] we noted a similar effect for Re.

In contrast with our approach, that of LTVC [13] and of [37] asks a more rigorous question: for a given compound, is there a temperature below melting where a single solid-solution phase is the thermodynamic equilibrium? This is a better phrased question, and could allow for systematic improvements. They predict both T_c, the lowest temperature where such a phase could exist, and make a reasonable estimate for the melting temperature. In section 2.2, we present a comparison of both [12] and of LTVC approaches, and see strengths and weaknesses in both. To make comparison easier, we re-formulated our criteria in terms of dimensionless enthalpies of formation, by normalizing by k_BT_m, using the LTVC estimate for T_m. For conciseness, we focus on the 1104 quaternary compounds they list. Of these, they predict 486 compounds that can form solid solutions below their estimated melting point. Our enthalpy approach is consistent with these in 201 cases, so the approaches actually disagree in more than half of the cases. In the cases where they disagree, 21 cases contain Al, which we have already noted poses issues for our approach. The LTVC approach appears to account for this more naturally, by specifically considering the enthalpy of the solid solution.

Of the cases where LTVC and our approach disagree, there are 158 cases (listed in Table 5 in Appendix 2) where an LTVC predicted solid solution has a pair of elements where we find $H/k_BT_m>0.3$, which our approach predicts will not form single phases. These cases are dominated by compounds containing Ag, Au and/or Cu. We note that [1] does not list any single-phase compounds containing these elements. Thus, in these cases, it appears that our approach seems more reliable. There are 160 cases (listed in Table 6) where an LTVC predicted solid solution has a pair of elements with $H/k_BT_m<-1.0$, which our approach predicts will form ordered phases. These cases are dominated by compounds with Re, which has issues with our approach as noted before. A number of remaining cases have Mo-Pt as the lowest enthalpy pair. The Mo-Pt phase diagram exhibits a wide composition range with an FCC solid-solution at elevated temperatures, suggesting that despite the low (strongly negative) formation enthalpy, there is a low driving force for ordering (as in a number of Al- and Re-containing binaries). In these cases, where our matrix does not fully account for the formation enthalpy of the solid solution phase, the LTVC approach appears to more naturally account for these, resulting in better predictions.

Overall, the differences between these suggest that neither approach is fully developed: the LTVC approach seeks to answer a more carefully phrased question for single-phase stability: is there a stable, solid solution phase below melting? The enthalpy approach has the weakness that in its present form, it usually only considers enthalpies of ordered phases, yet clearly the solid-solution enthalpy ought to be accounted for. If that enthalpy is strongly positive, then it will be unlikely to form a solid solution; on the other hand, if it is negative, then that is much more likely to form a solid solution, by reducing the driving force for ordering. Moreover, the approach considers the entropy in a very simple form: in [11, 12], the entropy was only by considering the annealing temperature and the ideal entropy of mixing, i.e. $T_{anneal}S_{ideal}$, to compare with the enthalpy of formation. Figure 1 shows an enthalpy window that makes no reference to temperature, thus eliminating the (clearly important) role of entropy. In Eq. 1, we normalize not by annealing temperature, but by the melting temperature (as estimated by [13]; see caption of Table 5 in that paper for the method). Thus, the enthalpy approach treats the entropy in a very simplistic way. A proper treatment would also include both more realistic interactions: the results for Al-Li-Ti compounds presented in section 3.2 have evidence of forming solid solutions despite both strongly positive (Li-Ti)

and strongly negative (Al-Ti) enthalpies. Clearly, there is room to incorporate more realistic estimates of the thermodynamic behaviors beyond simple enthalpy arguments and ideal entropies of mixing.

A clear and established way to systematically improve this beyond pair interactions is through the use of cluster expansions [30-33]. The cluster expansions provide a systematic approach to incorporate 3-body and higher order interactions. The challenge is that the number of parameters quickly become large, particularly for alloys with a large number of constituents. However, recently developed automated approaches [34] make the cluster expansion amenable to multicomponent systems, and these methods are being applied to examine ordering transitions in high entropy alloys (see, for example, [42], as well as the broader review in [43].

In section 3, we demonstrate simple approaches to utilize our enthalpy matrix in Monte Carlo simulations of Al-containing compounds. In contrast to the predictions of Al-containing single phases based on our minimum/maximum enthalpy criteria, these results show reasonable comparison with experimental data. We attribute this difference due to the fact that the minimum/maximum enthalpy criteria do not explicitly account for the enthalpy of the solid solution phase, which is a significant limitation, but that deriving interactions from this can lead to reasonable driving forces for ordering from a solid-solution phase, when solid-solution formation is reasonably competitive. This strongly suggests the importance of considering the enthalpy of solid solutions. The particular cases discussed in section 3 showcase some of these issues. For $Al_xCoCrFeNi$, the ordering temperature is strongly affected by the Al content, but the Monte Carlo appears to capture not only this trend, but also the degree of B2 ordering as a function of temperature [16]. It also provides important information on short-range ordering as a function of temperature, and further captures the experimentally observed evolution from a weakly-ordered B2 phase to a mixture of strongly ordered B2 phase (predominantly Ni-Co-Al) and BCC solid solution (predominantly Cr-Fe). We also present the first simulations of an Al-Li-Mg-Sc-Ti alloy that has been reported to form a single phase when mechanically alloyed [17]. Our simulations support the experimental observation, showing a single phase at reasonable temperatures, despite the strongly tendency of Al to form ordered alloys with the other components (particularly Sc and Ti), and despite the strong immiscibility of Li and Ti. In general, we find evidence that, in certain composition ranges, it is reasonable to form Al-Li-Ti alloys, with the Al-Li and Al-Ti interactions overcoming the Li-Ti repulsion. Thus, this approach has the potential to guide experiments on compounds that form challenges, such as Al-Li-Ti that cannot be easily formed through normal casting approaches.

Overall, these results show significant developments towards phase prediction in complex alloy systems. We envision that in the future, these approaches will be developed further, to become both more rigorous and more accurate. Accounting for solid-solution enthalpies is clearly important but not fully accounted for in our own approach [11, 12]. The LTVC approach clearly captures such effects better, thus providing more natural predictions of Al-containing single phase solid solutions. Beyond single phase predictions, Monte Carlo simulations also show (in some cases) the ability to utilize similar information, but predict short-range order, trends in phase stability, and potential phase transformations. Ultimately, we envision the development of much stronger, more rigorous methods that greatly enhance our ability to explore new alloy compositions from a first-principles basis.

Acknowledgements:

This work is primarily supported by the U.S. Department of Energy (DOE) Office of Science, Basic Energy Sciences, Materials Science and Engineering Division. Work on Al-Ti-Li compounds was supported through the DOE Office of Energy Efficiency and Renewable Energy, Advanced Manufacturing Office's HPC4Mfg program.

Data Availability:

The raw/processed data required to reproduce these findings cannot be shared at this time due to technical or time limitations. The primary data required to reproduce these studies come from Table 4, as well as data in references [1] and [13]. Monte Carlo studies on $Al_xCoCrFeNi$ are based on data from [16] and may be made available. Monte Carlo studies on Al-Li-Ti alloys form parts of on-going studies.

References

[1] M.C. Gao, C. Zhang, P. Gao, F. Zhang, L.Z. Ouyang, M. Widom, J.A. Hawk, Thermodynamics of concentrated solid solution alloys, Current Opinion in Solid State and Materials Science 21(5) (2017) 238-251.

[2] J.W. Yeh, S.K. Chen, S.J. Lin, J.Y. Gan, T.S. Chin, T.T. Shun, C.H. Tsau, S.Y. Chang, Nanostructured high-entropy alloys with multiple principal elements: Novel alloy design concepts and outcomes, Advanced Engineering Materials 6(5) (2004) 299-303.

[3] B. Cantor, I.T.H. Chang, P. Knight, A.J.B. Vincent, Microstructural development in equiatomic multicomponent alloys, Mat. Sci. Eng. A 375 (2004) 213-218.

[4] F. Otto, Y. Yang, H. Bei, E.P. George, Relative effects of enthalpy and entropy on the phase stability of equiatomic high-entropy alloys, Acta Mater. 61(7) (2013) 2628-2638.

[5] B. Gludovatz, A. Hohenwarter, D. Catoor, E.H. Chang, E.P. George, R.O. Ritchie, A fracture-resistant high-entropy alloy for cryogenic applications, Science 345(6201) (2014) 1153-1158.

[6] D.B. Miracle, O.N. Senkov, A critical review of high entropy alloys and related concepts, Acta Mater. 122 (2017) 448-511.

[7] O.N. Senkov, J.D. Miller, D.B. Miracle, C. Woodward, Accelerated exploration of multi-principal element alloys for structural applications, Calphad 50 (2015) 32-48.

[8] O.N. Senkov, G.B. Wilks, D.B. Miracle, C.P. Chuang, P.K. Liaw, Refractory high-entropy alloys, Intermetallics 18(9) (2010) 1758-1765.

[9] Z. Wu, M.C. Troparevsky, Y.F. Gao, J.R. Morris, G.M. Stocks, H. Bei, Phase stability, physical properties and strengthening mechanisms of concentrated solid solution alloys, Current Opinion in Solid State and Materials Science 21(5) (2017) 267-284.

[10] K. Jin, B.C. Sales, G.M. Stocks, G.D. Samolyuk, M. Daene, W.J. Weber, Y. Zhang, H. Bei, Tailoring the physical properties of Ni-based single-phase equiatomic alloys by modifying the chemical complexity, Scientific Reports 6 (2016) 20159.

[11] M.C. Troparevsky, J.R. Morris, M. Daene, Y. Wang, A.R. Lupini, G.M. Stocks, Beyond Atomic Sizes and Hume-Rothery Rules: Understanding and Predicting High-Entropy Alloys, Journal of the Minerals Metals & Materials Society (JOM) 67(10) (2015) 2350-2363.

[12] M.C. Troparevsky, J.R. Morris, P.R.C. Kent, A.R. Lupini, G.M. Stocks, Criteria for Predicting the Formation of Single-Phase High-Entropy Alloys, Physical Review X 5(1) (2015) 011041.

[13] Y. Lederer, C. Toher, K.S. Vecchio, S. Curtarolo, The search for high entropy alloys: A high-throughput ab-initio approach, Acta Mater. 159 (2018) 364-383.

[14] B. Schuh, F. Mendez-Martin, B. Völker, E.P. George, H. Clemens, R. Pippan, A. Hohenwarter, Mechanical properties, microstructure and thermal stability of a nanocrystalline CoCrFeMnNi high-entropy alloy after severe plastic deformation, Acta Mater. 96 (2015) 258-268.

[15] E.J. Pickering, R. Muñoz-Moreno, H.J. Stone, N.G. Jones, Precipitation in the equiatomic high-entropy alloy CrMnFeCoNi, Scr. Mater. 113 (2016) 106-109.

[16] L.J. Santodonato, P.K. Liaw, R.R. Unocic, H. Bei, J.R. Morris, Predictive multiphase evolution in Al-containing high-entropy alloys, Nat Commun 9(1) (2018) 4520.

[17] K.M. Youssef, A.J. Zaddach, C. Niu, D.L. Irving, C.C. Koch, A Novel Low-Density, High-Hardness, High-entropy Alloy with Close-packed Single-phase Nanocrystalline Structures, Materials Research Letters 3(2) (2015) 95-99.

[18] N.D. Stepanov, D.G. Shaysultanov, G.A. Salishchev, M.A. Tikhonovsky, Structure and mechanical properties of a light-weight AlNbTiV high entropy alloy, Materials Letters 142 (2015) 153-155.

[19] A. Zunger, S.H. Wei, L.G. Ferreira, J.E. Bernard, Special quasirandom structures, Phys. Rev. Lett. 65(3) (1990) 353-356.

[20] P. Singh, A.V. Smirnov, A. Alam, D.D. Johnson, First-principles prediction of incipient order in arbitrary high-entropy alloys: exemplified in Ti0.25CrFeNiAlx, Acta Mater. 189 (2020) 248-254.

[21] Y.Y. Ye, Y. Chen, K.M. Ho, B.N. Harmon, P.A. Lindgard, Phonon-Phonon Coupling and the Stability of the High-Temperature BCC Phase of Zr, Phys. Rev. Lett. 58(17) (1987) 1769-1772.

[22] J.R. Morris, R.J. Gooding, Vibrational Entropy Effects at a Diffusionless 1st-Order Solid-to-Solid Transition, Phys. Rev. B 43(7) (1991) 6057-6067.

[23] B. Fultz, Vibrational thermodynamics of materials, Prog. Mater. Sci. 55(4) (2010) 247-352.

[24] B. Fultz, L. Anthony, J.L. Robertson, R.M. Nicklow, S. Spooner, M. Mostoller, Phonon modes and vibrational entropy of mixing in Fe-Cr, Phys. Rev. B 52(5) (1995) 3280-3285.

[25] G.J. Ackland, Vibrational entropy of ordered and disordered alloys, Alloy Model. Des., Proc. Symp. (1994) 149-53.

[26] T.L. Swan-Wood, O. Delaire, B. Fultz, Vibrational entropy of spinodal decomposition in FeCr, Phys. Rev. B 72(2) (2005) 024305.

[27] F. Körmann, Y. Ikeda, B. Grabowski, M.H.F. Sluiter, Phonon broadening in high entropy alloys, npj Computational Materials 3(1) (2017) 36.

[28] S. Curtarolo, W. Setyawan, G.L.W. Hart, M. Jahnatek, R.V. Chepulskii, R.H. Taylor, S.D. Wanga, J.K. Xue, K.S. Yang, O. Levy, M.J. Mehl, H.T. Stokes, D.O. Demchenko, D. Morgan, AFLOW: An automatic framework for high-throughput materials discovery, Comput. Mater. Sci. 58 (2012) 218-226.

[29] M. Widom, Alloy Database. http://alloy.phys.cmu.edu/).

[30] A.V. Ruban, I.A. Abrikosov, Configurational thermodynamics of alloys from first principles: Effective cluster interactions, Reports on Progress in Physics 71(4) (2008).

[31] D.B. Laks, L.G. Ferreira, S. Froyen, A. Zunger, Efficient cluster expansion for substitutional systems, Phys. Rev. B 46(19) (1992) 12587-12605.

[32] D.D. Fontaine, Cluster Approach to Order-Disorder Transformations in Alloys, Solid State Physics - Advances in Research and Applications 47(C) (1994) 33-176.

[33] J.W.D. Connolly, A.R. Williams, Density-functional theory applied to phase transformations in transition-metal alloys, Phys. Rev. B 27(8) (1983) 5169-5172.

[34] A. Van de Walle, M. Asta, G. Ceder, The alloy theoretic automated toolkit: A user guide, Calphad: Computer Coupling of Phase Diagrams and Thermochemistry 26(4) (2002) 539-553.

[35] A. Sher, M. van Schilfgaarde, A.-B. Chen, W. Chen, Quasichemical approximation in binary alloys, Phys. Rev. B 36(8) (1987) 4279.

[36] M. Berding, A. Sher, Electronic quasichemical formalism: Application to arsenic deactivation in silicon, Phys. Rev. B 58(7) (1998) 3853.

[37] D.J.M. King, S.C. Middleburgh, A.G. McGregor, M.B. Cortie, Predicting the formation and stability of single phase high-entropy alloys, Acta Mater. 104 (2016) 172-179.

[38] F.R. De Boer, W. Mattens, R. Boom, A. Miedema, A. Niessen, Cohesion in metals, (1988).

[39] M. Gao, B. Schneiderman, S.M. Gilbert, Z. Yu, Microstructural Evolution and Mechanical Properties of Nickel-Base Superalloy Brazed Joints Using a MPCA Filler, Mat. Trans. A 50(11) (2019) 5117-5127.

[40] C.J. Tong, Y.L. Chen, S.K. Chen, J.W. Yeh, T.T. Shun, C.H. Tsau, S.J. Lin, S.Y. Chang, Microstructure characterization of $Al_xCoCrCuFeNi$ high-entropy alloy system with multiprincipal elements, Mat. Trans. A 36A(4) (2005) 881-893.

[41] L.J. Santodonato, Y. Zhang, M. Feygenson, C.M. Parish, M.C. Gao, R.J.K. Weber, J.C. Neuefeind, Z. Tang, P.K. Liaw, Deviation from high-entropy configurations in the atomic distributions of a multi-principal-element alloy, Nat Commun 6 (2015) 5964

[42] W.P. Huhn, M. Widom, Prediction of A2 to B2 Phase Transition in the High-Entropy Alloy Mo-Nb-Ta-W, JOM 65(12) (2013) 1772-1779.

[43] M. Widom, Modeling the structure and thermodynamics of high-entropy alloys, Journal of Materials Research 33(19) (2018) 2881-2898.

Appendix 1.

Table 4. Enthalpy matrix, in meV/atom. Each entry represents the first-principles energy of the lowest known compound, relative to the lowest-energy pure phases. These are extracted primarily from the AFLOW database [28] and also from [29]. We note that some values, in particular for Fe-Mo, differ from those in [12]. The case Cr-Ti was discussed explicitly in [12], as the databases at that time did not consider certain crystal structures that are now included. This matrix has updated data for Cr-Ti, Cr-Zr, and Cr-Hf from the AFLOW database.

Element	Mg	Al	Sc	Ti	V	Cr	Mn	Fe	Co	Ni	Cu	Zn	Y	Zr	Nb	Mo	Ru	Rh	Pd	Ag	Cd	La	Hf	Ta	W	Re	Os	Ir	Pt	Au
Mg	0	-33	2	20	171	160	87	77	-31	-723	-147	-139	4	-31	105	164	4	-478	-742	-255	-109	-140	-7	122	234	67	43	-369	-872	-612
Al	-33	0	-444	-428	-282	-138	-278	-369	-629	-677	-224	-520	-544	-539	-288	-168	-678	-1101	-874	-254	-1938	-360	-444	-320	-161	-257	-577	-944	-960	-466
Sc	2	-444	0	38	83	119	-142	-281	-359	-525	-284	-380	18	-29	61	-11	-540	-1035	-906	-309	-296	33	-10	75	44	-341	-400	-1032	-1232	-822
Ti	20	-428	38	0	37	-120.878	-277	-418	-386	-435	-147	-198	111	24	11	-167	-763	-790	-646	-65	-69	134	-10	31	-82	-189	-713	-847	-934	-430
V	171	-282	83	37	0	-88	-286	-176	-199	-250	13	-51	143	26	-56	-127	-321	-393	-275	147	133	170	7	-122	-97	-148	-361	-505	-564	-43
Cr	160	-138	119	-120.878	-88	0	-110	-8	5	-30	108	44	150	-48.1282	-47	42	4	-129	-82	129	133	173	-119	-130	26	4	-22	-238	-261	25
Mn	87	-278	-142	-277	-286	-110	0	9	-19	-115	29	-25	40	-192	-153	-138	-15	-188	-251	97	90	129	-268	-254	-92	-139	-40	-199	-362	-111
Fe	77	-369	-281	-418	-176	-8	9	0	-60	-97	65	-23	-71	-290	-2505	-484	41	-57	-116	176	159	18	-354	-3468	-554	-25	11	-63	-244	70
Co	-31	-629	-359	-386	-199	5	-19	-60	0	-21	54	-58	-198	-324	-178	-52	52	12	-10	154	134	-128	-401	-253	-84	-72	34	3	-107	84
Ni	-723	-677	-525	-435	-250	-30	-115	-97	-21	0	-6	-256	-437	-463	-316	-100	40	2	-6	98	-14	-339	-544	-746	-116	-116	32	-38	-99	44
Cu	-147	-224	-284	-147	54	108	29	65	54	-6	0	-92	-258	-169	-29	83	108	-4	-126	47	3	-229	-186	28	129	83	141	24	-167	-49
Zn	-139	-520	-380	-198	-51	44	-25	-23	-58	-256	-92	0	-405	-301	-160	-42	-150	-391	-571	-62	32	-374	-233	-88	58	8	21	-238	-570	-222
Y	4	-544	18	111	143	150	40	-71	-198	-437	-258	-405	0	40	143	100	-318	-863	-923	-346	-358	3	65	181	148	-211	-304	-804	-1252	-889
Zr	-31	-539	-29	24	26	-48.1282	-192	-290	-324	-463	-169	-301	40	0	21	-138	-644	-811	-816	-126	-123	99	-22	36	-145	-358	-524	-830	-1087	-580
Nb	105	-288	61	11	-56	-47	-153	-2505	-150	-316	-29	-160	143	21	0	-133	-249	-548	-435	70	71	145	23	-10	-76	-202	-276	-628	-721	-157
Mo	164	-168	-11	-167	-127	42	-136	-484	-52	-100	83	-42	100	-138	-133	0	-57	-248	-100	238	176	212	-171	-193	-8	-2	-52	-338	-366	141
Ru	4	-678	-540	-763	-321	4	-15	41	52	40	108	-150	-318	-644	-249	-57	0	-8	47	203	112	-290	-819	-332	-66	-87	-16	-54	-33	162
Rh	-478	-1101	-1035	-790	-393	-129	-188	-57	12	2	-4	-391	-863	-811	-548	-248	-8	0	37	80	-162	-790	-864	-611	-273	-181	-8	-21	-24	76
Pd	-742	-874	-906	-646	-275	-82	-251	-116	-10	-6	-126	-571	-923	-816	-435	-100	47	37	0	-63	-419	-838	-879	-480	-123	-57	67	40	-36	-95
Ag	-255	-76	-309	-65	147	129	97	176	154	98	47	-62	-346	-126	70	238	203	80	-63	0	-66	-307	-122	107	331	178	257	171	-39	-85
Cd	-109	-1938	-296	-69	133	113	90	159	134	-14	3	32	-358	-123	71	176	112	-162	-419	-66	0	-381	-84	94	286	154	220	23	-320	-182
La	-140	-360	33	170	170	173	129	18	-128	-339	-229	-374	3	99	145	212	-290	-790	-838	-307	-381	0	114	166	299	76	-162	-735	-1198	-837
Hf	-7	-444	-10	-10	7	-119	-268	-354	-401	-544	-186	-233	65	-22	23	-171	-819	-864	-879	-122	-84	114	0	49	-171	-407	-709	-949	-1155	-566
Ta	122	-320	75	31	-122	-130	-254	-3468	-253	-746	28	-88	181	36	-10	-193	-332	-611	-480	107	94	166	49	0	-114	-226	-330	-688	-758	-93
W	234	-161	44	-82	-97	26	-92	-554	-84	-116	129	58	148	-145	-76	-8	-66	-273	-123	331	286	299	-171	-114	0	7	-56	-350	-343	232
Re	67	-257	-341	-189	-148	4	-139	-25	-72	-116	83	8	-211	-358	-202	-2	-87	-181	-57	178	154	76	-407	-226	7	0	-89	-274	-232	166
Os	43	-577	-400	-713	-361	-22	-40	11	34	32	141	21	-304	-524	-276	-52	-16	-8	67	257	220	-162	-709	-330	-56	-89	0	-8	22	232
Ir	-369	-944	-1032	-847	-505	-238	-199	-63	3	-38	24	-238	-804	-830	-830	-338	-54	-21	40	171	23	-735	-949	-688	-350	-274	-8	0	11	154
Pt	-872	-960	-1232	-934	-564	-261	-362	-244	-107	-99	-167	-570	-1252	-1087	-721	-366	-33	-24	-36	-39	-320	-1198	-1155	-758	-343	-232	22	11	0	8
Au	-612	-466	-822	-430	-43	25	-111	70	84	44	-49	-222	-889	-580	-157	141	162	76	-95	-85	-182	-837	-566	-93	232	166	232	154	8	0

Appendix 2.

Table 5. Quaternary compounds predicted to be single phase by LTVC [13] according to the criterion $T_c/T_m<1.0$, but predicted to be multiple phase by $H_{max}/k_BT_m>0.3$ (see Eq. 1). Here, T_c is the LTVC predicted lowest temperature for a single phase solid solution, T_m is the estimated melting temperature from [13]. The "Minimum pair" is the pair of elements within the compound with the lowest formation enthalpy H_{min}, and the "maximum pair" is the pair with the highest formation enthalpy H_{max}.

Compound	T_c (K)	T_m (K)	T_c/T_m	Minimum pair	H_{min} (meV)	H_{min}/k_BT_m	Maximum pair	H_{max} (meV)	H_{max}/k_BT_m
AgAlAuCu	980	1220	0.80	Al, Au	-466	-4.43	Ag, Cu	47	0.45
AgAuCoIr	340	1760	0.19	Ag, Au	-85	-0.56	Ag, Ir	171	1.13
AgAuCoNi	420	1470	0.29	Ag, Au	-85	-0.67	Ag, Co	154	1.22
AgAuCoRh	1080	1640	0.66	Ag, Au	-85	-0.60	Ag, Co	154	1.09
AgAuCrNi	660	1610	0.41	Ag, Au	-85	-0.61	Ag, Cr	129	0.93
AgAuCuFe	1040	1430	0.73	Ag, Au	-85	-0.69	Ag, Fe	176	1.43
AgAuCuNi	600	1350	0.44	Ag, Au	-85	-0.73	Ag, Ni	98	0.84
AgAuCuPd	980	1380	0.71	Cu, Pd	-126	-1.06	Ag, Cu	47	0.40
AgAuFePd	1480	1550	0.95	Fe, Pd	-116	-0.87	Ag, Fe	176	1.32
AgAuFeRh	740	1650	0.45	Ag, Au	-85	-0.60	Ag, Fe	176	1.24
AgAuIrPd	260	1770	0.15	Au, Pd	-95	-0.62	Ag, Ir	171	1.12
AgAuIrPt	960	1830	0.52	Ag, Au	-85	-0.54	Ag, Ir	171	1.08
AgAuMoPd	1180	1820	0.65	Mo, Pd	-100	-0.64	Ag, Mo	238	1.52
AgAuNiRe	780	1940	0.40	Ni, Re	-116	-0.69	Ag, Re	178	1.06
AgAuNiRh	1040	1630	0.64	Ag, Au	-85	-0.61	Ag, Ni	98	0.70
AgAuPdRe	420	1960	0.21	Au, Pd	-95	-0.56	Ag, Re	178	1.05
AgAuPdRu	280	1750	0.16	Au, Pd	-95	-0.63	Ag, Ru	203	1.35
AgAuPtRh	740	1710	0.43	Ag, Au	-85	-0.58	Ag, Rh	80	0.54
AgAuPtRu	1620	1800	0.90	Ag, Au	-85	-0.55	Ag, Ru	203	1.31
AgAuRhRu	540	1850	0.29	Ag, Au	-85	-0.53	Ag, Ru	203	1.27
AgCoIrPd	280	1880	0.15	Ag, Pd	-63	-0.39	Ag, Ir	171	1.06
AgCoIrPt	1660	1930	0.86	Co, Pt	-107	-0.64	Ag, Ir	171	1.03
AgCoMoPd	1140	1930	0.59	Mo, Pd	-100	-0.60	Ag, Mo	238	1.43
AgCoNiPd	680	1550	0.44	Ag, Pd	-63	-0.47	Ag, Co	154	1.15
AgCoPdPt	1420	1620	0.88	Co, Pt	-107	-0.77	Ag, Co	154	1.10
AgCoPdRe	960	2070	0.46	Co, Re	-72	-0.40	Ag, Re	178	1.00
AgCoPdRh	1400	1770	0.79	Ag, Pd	-63	-0.41	Ag, Co	154	1.01
AgCoPtRe	1020	2130	0.48	Pt, Re	-232	-1.26	Ag, Re	178	0.97
AgCoPtRh	1260	1820	0.69	Co, Pt	-107	-0.68	Ag, Co	154	0.98
AgCrIrRu	460	2160	0.21	Cr, Ir	-238	-1.28	Ag, Ru	203	1.09
AgCrPtRu	460	2000	0.23	Cr, Pt	-261	-1.51	Ag, Ru	203	1.18
AgCrRhRu	240	2050	0.12	Cr, Rh	-129	-0.73	Ag, Ru	203	1.15

AgCuFeOs	1120	1930	0.58	Fe, Os	11	0.07	Ag, Os	257	1.55
AgCuFePd	1420	1530	0.93	Cu, Pd	-126	-0.96	Ag, Fe	176	1.33
AgCuNiPd	1480	1480	1.00	Cu, Pd	-126	-0.99	Ag, Ni	98	0.77
AgCuPdPt	1380	1590	0.87	Cu, Pt	-167	-1.22	Ag, Cu	47	0.34
AgFeMoOs	1320	2310	0.57	Mo, Os	-52	-0.26	Ag, Os	257	1.29
AgFeMoPd	720	1940	0.37	Fe, Pd	-116	-0.69	Ag, Mo	238	1.42
AgFeMoRe	1440	2350	0.61	Fe, Re	-25	-0.12	Ag, Mo	238	1.18
AgFeNiPd	700	1650	0.42	Fe, Pd	-116	-0.82	Ag, Fe	176	1.24
AgFeOsRe	1360	2450	0.56	Os, Re	-89	-0.42	Ag, Os	257	1.22
AgFeOsRu	1360	2240	0.61	Os, Ru	-16	-0.08	Ag, Os	257	1.33
AgFePdRh	720	1780	0.40	Fe, Pd	-116	-0.76	Ag, Fe	176	1.15
AgFeReRu	1280	2270	0.56	Re, Ru	-87	-0.44	Ag, Ru	203	1.04
AgIrNiPd	1240	1870	0.66	Ag, Pd	-63	-0.39	Ag, Ir	171	1.06
AgIrNiPt	1620	1920	0.84	Ni, Pt	-99	-0.60	Ag, Ir	171	1.03
AgIrOsPd	440	2270	0.19	Ag, Pd	-63	-0.32	Ag, Os	257	1.31
AgIrPdRu	420	2080	0.20	Ag, Pd	-63	-0.35	Ag, Ru	203	1.13
AgIrPtRe	1040	2350	0.44	Ir, Re	-274	-1.35	Ag, Re	178	0.88
AgIrPtRh	380	2050	0.19	Ag, Pt	-39	-0.22	Ag, Ir	171	0.97
AgIrPtRu	1240	2140	0.58	Ir, Ru	-54	-0.29	Ag, Ru	203	1.10
AgMoNiRu	780	2110	0.37	Mo, Ni	-100	-0.55	Ag, Mo	238	1.31
AgMoOsRe	1600	2720	0.59	Os, Re	-89	-0.38	Ag, Os	257	1.10
AgMoPdRe	1740	2350	0.74	Mo, Pd	-100	-0.49	Ag, Mo	238	1.18
AgNiOsPd	460	2030	0.23	Ag, Pd	-63	-0.36	Ag, Os	257	1.47
AgNiPdPt	1580	1700	0.93	Ni, Pt	-99	-0.68	Ag, Ni	98	0.67
AgNiPdRe	1960	2060	0.95	Ni, Re	-116	-0.65	Ag, Re	178	1.00
AgNiPdRh	720	1760	0.41	Ag, Pd	-63	-0.42	Ag, Ni	98	0.65
AgNiPtRe	920	2110	0.44	Pt, Re	-232	-1.28	Ag, Re	178	0.98
AgNiPtRh	1200	1810	0.66	Ni, Pt	-99	-0.63	Ag, Ni	98	0.63
AgNiPtRu	560	1900	0.29	Ni, Pt	-99	-0.60	Ag, Ru	203	1.24
AgOsPdRe	960	2460	0.39	Os, Re	-89	-0.42	Ag, Os	257	1.21
AgOsPdRh	480	2150	0.22	Ag, Pd	-63	-0.34	Ag, Os	257	1.39
AgOsPdRu	740	2240	0.33	Ag, Pd	-63	-0.33	Ag, Os	257	1.33
AgOsPtRe	760	2510	0.30	Pt, Re	-232	-1.07	Ag, Os	257	1.19
AgOsPtRh	1380	2210	0.62	Ag, Pt	-39	-0.20	Ag, Os	257	1.35
AgOsPtRu	760	2300	0.33	Ag, Pt	-39	-0.20	Ag, Os	257	1.30
AgPdPtRe	1720	2140	0.80	Pt, Re	-232	-1.26	Ag, Re	178	0.97
AgPdPtRu	1140	1920	0.59	Ag, Pd	-63	-0.38	Ag, Ru	203	1.23
AgPdReRh	720	2190	0.33	Re, Rh	-181	-0.96	Ag, Re	178	0.94
AgPdRhRu	540	1970	0.27	Ag, Pd	-63	-0.37	Ag, Ru	203	1.20
AgPtReRh	1140	2240	0.51	Pt, Re	-232	-1.20	Ag, Re	178	0.92
AgPtReRu	540	2330	0.23	Pt, Re	-232	-1.16	Ag, Ru	203	1.01

AgPtRhRu	820	2030	0.40	Ag, Pt	-39	-0.22	Ag, Ru	203	1.16
AlCuFeNi	1380	1580	0.87	Al, Ni	-677	-4.97	Cu, Fe	65	0.48
AuCoCrPd	720	1770	0.41	Au, Pd	-95	-0.62	Au, Co	84	0.55
AuCoIrPd	640	1900	0.34	Au, Pd	-95	-0.58	Au, Ir	154	0.94
AuCoMoPd	1200	1960	0.61	Mo, Pd	-100	-0.59	Au, Mo	141	0.83
AuCoNiPd	520	1530	0.34	Au, Pd	-95	-0.72	Au, Co	84	0.64
AuCuFePd	1320	1580	0.84	Cu, Pd	-126	-0.93	Au, Fe	70	0.51
AuCuPdRe	460	1990	0.23	Cu, Pd	-126	-0.73	Au, Re	166	0.97
AuCuPdRu	500	1780	0.28	Cu, Pd	-126	-0.82	Au, Ru	162	1.06
AuCuPtRe	760	2050	0.37	Pt, Re	-232	-1.31	Au, Re	166	0.94
AuCuPtRu	1520	1830	0.83	Cu, Pt	-167	-1.06	Au, Ru	162	1.03
AuFeNiPd	940	1670	0.56	Fe, Pd	-116	-0.81	Au, Fe	70	0.49
AuFePdRe	540	2110	0.26	Fe, Pd	-116	-0.64	Au, Re	166	0.91
AuIrNiPd	980	1890	0.52	Au, Pd	-95	-0.58	Au, Ir	154	0.95
AuIrOsPd	500	2290	0.22	Au, Pd	-95	-0.48	Au, Os	232	1.18
AuIrOsPt	940	2350	0.40	Ir, Os	-8	-0.04	Au, Os	232	1.15
AuIrPdPt	340	1970	0.17	Au, Pd	-95	-0.56	Au, Ir	154	0.91
AuIrPdRh	540	2020	0.27	Au, Pd	-95	-0.55	Au, Ir	154	0.88
AuIrPdRu	800	2110	0.38	Au, Pd	-95	-0.52	Au, Ru	162	0.89
AuIrPtRh	380	2080	0.18	Pt, Rh	-24	-0.13	Au, Ir	154	0.86
AuIrPtRu	1420	2160	0.66	Ir, Ru	-54	-0.29	Au, Ru	162	0.87
AuMoNiPd	660	1950	0.34	Mo, Pd	-100	-0.60	Au, Mo	141	0.84
AuMoPdRe	1440	2380	0.61	Mo, Pd	-100	-0.49	Au, Re	166	0.81
AuMoPdRu	1260	2160	0.58	Mo, Pd	-100	-0.54	Au, Ru	162	0.87
AuMoPtRh	340	2130	0.16	Mo, Pt	-366	-1.99	Au, Mo	141	0.77
AuNiOsPd	560	2050	0.27	Au, Pd	-95	-0.54	Au, Os	232	1.31
AuNiPdRu	620	1870	0.33	Au, Pd	-95	-0.59	Au, Ru	162	1.01
AuNiPtRe	2100	2140	0.98	Pt, Re	-232	-1.26	Au, Re	166	0.90
AuOsPdPt	1060	2130	0.50	Au, Pd	-95	-0.52	Au, Os	232	1.26
AuOsPdRe	1020	2480	0.41	Au, Pd	-95	-0.44	Au, Os	232	1.09
AuOsPdRh	780	2180	0.36	Au, Pd	-95	-0.51	Au, Os	232	1.24
AuOsPtRh	1080	2230	0.48	Pt, Rh	-24	-0.12	Au, Os	232	1.21
AuPdPtRe	460	2170	0.21	Pt, Re	-232	-1.24	Au, Re	166	0.89
AuPdPtRu	1680	1950	0.86	Au, Pd	-95	-0.57	Au, Ru	162	0.96
AuPdReRh	900	2210	0.41	Re, Rh	-181	-0.95	Au, Re	166	0.87
AuPdReRu	980	2300	0.43	Au, Pd	-95	-0.48	Au, Re	166	0.84
AuPdRhRu	940	2000	0.47	Au, Pd	-95	-0.55	Au, Ru	162	0.94
AuPtReRu	1300	2350	0.55	Pt, Re	-232	-1.15	Au, Re	166	0.82
AuPtRhRu	600	2050	0.29	Pt, Ru	-33	-0.19	Au, Ru	162	0.92
CoCuNiPt	840	1700	0.49	Cu, Pt	-167	-1.14	Co, Cu	54	0.37
CoCuPdPt	1640	1670	0.98	Cu, Pt	-167	-1.16	Co, Cu	54	0.38

CoCuPdRe	1440	2100	0.69	Cu, Pd	-126	-0.70	Cu, Re	83	0.46
CoCuPtRe	960	2160	0.44	Pt, Re	-232	-1.25	Cu, Re	83	0.45
CoCuPtRh	1560	1770	0.88	Cu, Pt	-167	-1.09	Co, Cu	54	0.35
CoIrOsPd	580	2400	0.24	Co, Pd	-10	-0.05	Os, Pd	67	0.32
CoOsPdRe	1220	2590	0.47	Os, Re	-89	-0.40	Os, Pd	67	0.30
CoOsPdRh	1920	2290	0.84	Co, Pd	-10	-0.05	Os, Pd	67	0.34
CoOsPdRu	1880	2370	0.79	Os, Ru	-16	-0.08	Os, Pd	67	0.33
CrCuOsPd	760	2160	0.35	Cu, Pd	-126	-0.68	Cu, Os	141	0.76
CrCuOsPt	480	2210	0.22	Cr, Pt	-261	-1.37	Cu, Os	141	0.74
CrFeOsPd	1900	2270	0.84	Fe, Pd	-116	-0.59	Os, Pd	67	0.34
CrNiOsPd	1600	2250	0.71	Cr, Pd	-82	-0.42	Os, Pd	67	0.35
CuFeOsPd	740	2080	0.36	Cu, Pd	-126	-0.70	Cu, Os	141	0.79
CuFePdRe	1160	2110	0.55	Cu, Pd	-126	-0.69	Cu, Re	83	0.46
CuIrOsPd	480	2300	0.21	Cu, Pd	-126	-0.64	Cu, Os	141	0.71
CuNbTiV	1860	1960	0.95	Cu, Ti	-147	-0.87	Cu, V	54	0.32
CuNiOsPd	1220	2060	0.59	Cu, Pd	-126	-0.71	Cu, Os	141	0.79
CuNiOsPt	920	2110	0.44	Cu, Pt	-167	-0.92	Cu, Os	141	0.78
CuNiPdRe	1880	2090	0.90	Cu, Pd	-126	-0.70	Cu, Re	83	0.46
CuNiPtRe	1640	2150	0.76	Pt, Re	-232	-1.25	Cu, Re	83	0.45
CuNiPtRu	1160	1930	0.60	Cu, Pt	-167	-1.00	Cu, Ru	108	0.65
CuOsPdPt	360	2140	0.17	Cu, Pt	-167	-0.91	Cu, Os	141	0.76
CuOsPtRe	980	2540	0.39	Pt, Re	-232	-1.06	Cu, Os	141	0.64
CuOsPtRh	1880	2240	0.84	Cu, Pt	-167	-0.87	Cu, Os	141	0.73
CuOsPtRu	1320	2330	0.57	Cu, Pt	-167	-0.83	Cu, Os	141	0.70
CuPdPtRe	900	2170	0.41	Pt, Re	-232	-1.24	Cu, Re	83	0.44
CuPdPtRu	280	1950	0.14	Cu, Pt	-167	-0.99	Cu, Ru	108	0.64
CuPdReRh	860	2220	0.39	Re, Rh	-181	-0.95	Cu, Re	83	0.43
CuPdRhRu	420	2000	0.21	Cu, Pd	-126	-0.73	Cu, Ru	108	0.63
CuPtReRh	780	2270	0.34	Pt, Re	-232	-1.19	Cu, Re	83	0.42
CuPtReRu	880	2360	0.37	Pt, Re	-232	-1.14	Cu, Ru	108	0.53
CuPtRhRu	1560	2060	0.76	Cu, Pt	-167	-0.94	Cu, Ru	108	0.61
FeIrOsPd	880	2410	0.37	Fe, Pd	-116	-0.56	Os, Pd	67	0.32
FeOsPdRh	2040	2300	0.89	Fe, Pd	-116	-0.59	Os, Pd	67	0.34
FeOsPdRu	920	2380	0.39	Fe, Pd	-116	-0.57	Os, Pd	67	0.33
IrNiOsPd	1120	2390	0.47	Ir, Ni	-38	-0.18	Os, Pd	67	0.33
MnOsPdRu	1080	2310	0.47	Mn, Pd	-251	-1.26	Os, Pd	67	0.34
MoNiOsPd	2020	2030	1.00	Mo, Pd	-100	-0.57	Os, Pd	67	0.38
MoOsPdPt	1280	2190	0.58	Mo, Pt	-366	-1.94	Os, Pd	67	0.36
MoOsPdRh	1600	2570	0.62	Mo, Rh	-248	-1.12	Os, Pd	67	0.30
NiOsPdRe	1560	2580	0.60	Ni, Re	-116	-0.52	Os, Pd	67	0.30
NiOsPdRh	1220	2280	0.54	Os, Rh	-8	-0.04	Os, Pd	67	0.34

NiOsPdRu	960	2360	0.41	Os, Ru	-16	-0.08	Os, Pd	67	0.33
OsPdPtRh	1340	2360	0.57	Pd, Pt	-36	-0.18	Os, Pd	67	0.33
OsPdPtRu	580	2440	0.24	Pd, Pt	-36	-0.17	Os, Pd	67	0.32

Table 6. Quaternary compounds predicted to be single phase by LTVC [13] according to the criterion $T_c/T_m<1.0$, but predicted to form ordered compounds by $H_{max}/k_BT_m < -1.0$ (see Eq. 1). Here, T_c is the LTVC predicted lowest temperature for a single phase solid solution, T_m is the estimated melting temperature from [13]. The "Minimum pair" is the pair of elements within the compound with the lowest formation enthalpy H_{min}, and the "maximum pair" is the pair with the highest formation enthalpy H_{max}.

Compound	T_c (K)	T_m (K)	T_c/T_m	Minimum pair	H_{min}	H_{min}/k_bT_m	Maximum pair	H_{max}, meV	H_{max}/k_bT_m
AgAlAuCu	980	1220	0.80	Al, Au	-466	-4.43	Ag, Cu	47	0.45
AgAuCuPd	980	1380	0.71	Cu, Pd	-126	-1.06	Ag, Cu	47	0.40
AgCoPtRe	1020	2130	0.48	Pt, Re	-232	-1.26	Ag, Re	178	0.97
AgCrIrRu	460	2160	0.21	Cr, Ir	-238	-1.28	Ag, Ru	203	1.09
AgCrPtRu	460	2000	0.23	Cr, Pt	-261	-1.51	Ag, Ru	203	1.18
AgCuPdPt	1380	1590	0.87	Cu, Pt	-167	-1.22	Ag, Cu	47	0.34
AgIrPtRe	1040	2350	0.44	Ir, Re	-274	-1.35	Ag, Re	178	0.88
AgNiPtRe	920	2110	0.44	Pt, Re	-232	-1.28	Ag, Re	178	0.98
AgOsPtRe	760	2510	0.30	Pt, Re	-232	-1.07	Ag, Os	257	1.19
AgPdPtRe	1720	2140	0.80	Pt, Re	-232	-1.26	Ag, Re	178	0.97
AgPtReRh	1140	2240	0.51	Pt, Re	-232	-1.20	Ag, Re	178	0.92
AgPtReRu	540	2330	0.23	Pt, Re	-232	-1.16	Ag, Ru	203	1.01
AlCrFeRe	2080	2080	1.00	Al, Fe	-369	-2.06	Cr, Re	4	0.02
AlCrHfTi	1740	1860	0.94	Al, Hf	-444	-2.77	Hf, Ti	-10	-0.06
AlCrMoRe	1260	2220	0.57	Al, Re	-257	-1.34	Cr, Mo	42	0.22
AlCrMoTi	1860	1920	0.97	Al, Ti	-428	-2.59	Cr, Mo	42	0.25
AlCrMoV	1260	2050	0.61	Al, V	-282	-1.60	Cr, Mo	42	0.24
AlCrReV	1600	2180	0.73	Al, V	-282	-1.50	Cr, Re	4	0.02
AlCrReW	2140	2340	0.91	Al, Re	-257	-1.27	Cr, W	26	0.13
AlCrTiW	1860	1960	0.95	Al, Ti	-428	-2.53	Cr, W	26	0.15
AlCrVW	1440	2120	0.68	Al, V	-282	-1.54	Cr, W	26	0.14
AlCuFeNi	1380	1580	0.87	Al, Ni	-677	-4.97	Cu, Fe	65	0.48
AlHfTiV	1660	1900	0.87	Al, Hf	-444	-2.71	Ti, V	37	0.23
AlHfTiW	1380	2120	0.65	Al, Hf	-444	-2.43	Hf, Ti	-10	-0.05
AlMnTiV	1280	1730	0.74	Al, Ti	-428	-2.87	Ti, V	37	0.25
AlMoTiV	1280	2040	0.63	Al, Ti	-428	-2.43	Ti, V	37	0.21
AlMoVW	1100	2340	0.47	Al, V	-282	-1.40	Mo, W	-8	-0.04
AlNbTiV	1260	1970	0.64	Al, Ti	-428	-2.52	Ti, V	37	0.22
AlNbVW	580	2240	0.26	Al, Nb	-288	-1.49	Nb, V	-56	-0.29
AlReVW	1720	2410	0.71	Al, V	-282	-1.36	Re, W	7	0.03
AlTiVW	1760	2050	0.86	Al, Ti	-428	-2.42	Ti, V	37	0.21
AuCrPdPt	560	1830	0.31	Cr, Pt	-261	-1.66	Au, Cr	25	0.16
AuCuPtRe	760	2050	0.37	Pt, Re	-232	-1.31	Au, Re	166	0.94
AuCuPtRu	1520	1830	0.83	Cu, Pt	-167	-1.06	Au, Ru	162	1.03

AuMoPtRh	340	2130	0.16	Mo, Pt	-366	-1.99	Au, Mo	141	0.77
AuNiPtRe	2100	2140	0.98	Pt, Re	-232	-1.26	Au, Re	166	0.90
AuPdPtRe	460	2170	0.21	Pt, Re	-232	-1.24	Au, Re	166	0.89
AuPtReRu	1300	2350	0.55	Pt, Re	-232	-1.15	Au, Re	166	0.82
CoCrMoNb	1740	2040	0.85	Co, Nb	-178	-1.01	Cr, Mo	42	0.24
CoCrPtRu	1860	2130	0.87	Cr, Pt	-261	-1.42	Co, Ru	52	0.28
CoCuNiPt	840	1700	0.49	Cu, Pt	-167	-1.14	Co, Cu	54	0.37
CoCuPdPt	1640	1670	0.98	Cu, Pt	-167	-1.16	Co, Cu	54	0.38
CoCuPtRe	960	2160	0.44	Pt, Re	-232	-1.25	Cu, Re	83	0.45
CoCuPtRh	1560	1770	0.88	Cu, Pt	-167	-1.09	Co, Cu	54	0.35
CoIrPdRe	2000	2430	0.82	Ir, Re	-274	-1.31	Ir, Pd	40	0.19
CoIrPtRe	2440	2490	0.98	Ir, Re	-274	-1.28	Ir, Pt	11	0.05
CoMoOsPt	1180	2510	0.47	Mo, Pt	-366	-1.69	Co, Os	34	0.16
CoMoPtRe	1740	2540	0.69	Mo, Pt	-366	-1.67	Mo, Re	-2	-0.01
CoMoPtRh	1980	2030	0.98	Mo, Pt	-366	-2.09	Co, Rh	12	0.07
CoMoPtRu	2240	2320	0.97	Mo, Pt	-366	-1.83	Co, Ru	52	0.26
CoNiPtRe	1620	2250	0.72	Pt, Re	-232	-1.20	Co, Ni	-21	-0.11
CoOsPtRe	900	2650	0.34	Pt, Re	-232	-1.02	Co, Os	34	0.15
CoPdPtRe	1000	2270	0.44	Pt, Re	-232	-1.19	Co, Pd	-10	-0.05
CoPtReRh	980	2380	0.41	Pt, Re	-232	-1.13	Co, Rh	12	0.06
CoPtReRu	1420	2460	0.58	Pt, Re	-232	-1.09	Co, Ru	52	0.25
CrCuOsPt	480	2210	0.22	Cr, Pt	-261	-1.37	Cu, Os	141	0.74
CrFeMnV	1720	1800	0.96	Mn, V	-286	-1.84	Fe, Mn	9	0.06
CrFeNiV	1420	1740	0.82	Ni, V	-250	-1.67	Cr, Fe	-8	-0.05
CrIrOsPt	1880	2540	0.74	Cr, Pt	-261	-1.19	Os, Pt	22	0.10
CrIrPdRh	1440	2030	0.71	Cr, Ir	-238	-1.36	Ir, Pd	40	0.23
CrIrPtRh	1660	2190	0.76	Cr, Pt	-261	-1.38	Ir, Pt	11	0.06
CrIrPtRu	1540	2360	0.65	Cr, Pt	-261	-1.28	Ir, Pt	11	0.05
CrMnReV	1440	2080	0.69	Mn, V	-286	-1.60	Cr, Re	4	0.02
CrMnVW	2240	2370	0.95	Mn, V	-286	-1.40	Cr, W	26	0.13
CrNbReTi	2200	2220	0.99	Nb, Re	-202	-1.06	Nb, Ti	11	0.06
CrNiReV	1700	2050	0.83	Ni, V	-250	-1.42	Cr, Re	4	0.02
CrOsPtRh	1340	2430	0.55	Cr, Pt	-261	-1.25	Os, Pt	22	0.11
CrPtRhRu	1800	2250	0.80	Cr, Pt	-261	-1.35	Cr, Ru	4	0.02
CrReTiV	1680	2190	0.77	Re, Ti	-189	-1.00	Ti, V	37	0.20
CuNbPdRh	900	2040	0.44	Nb, Rh	-548	-3.12	Pd, Rh	37	0.21
CuNiPdPt	1240	1640	0.76	Cu, Pt	-167	-1.18	Ni, Pd	-6	-0.04
CuNiPtRe	1640	2150	0.76	Pt, Re	-232	-1.25	Cu, Re	83	0.45
CuNiPtRh	1640	1760	0.93	Cu, Pt	-167	-1.10	Ni, Rh	2	0.01
CuNiPtRu	1160	1930	0.60	Cu, Pt	-167	-1.00	Cu, Ru	108	0.65
CuOsPtRe	980	2540	0.39	Pt, Re	-232	-1.06	Cu, Os	141	0.64

CuPdPtRe	900	2170	0.41	Pt, Re	-232	-1.24	Cu, Re	83	0.44
CuPtReRh	780	2270	0.34	Pt, Re	-232	-1.19	Cu, Re	83	0.42
CuPtReRu	880	2360	0.37	Pt, Re	-232	-1.14	Cu, Ru	108	0.53
FeMnReTi	1040	2180	0.48	Fe, Ti	-418	-2.23	Fe, Mn	9	0.05
FeMnReV	1740	2240	0.78	Mn, V	-286	-1.48	Fe, Mn	9	0.05
FeMnVW	2120	2290	0.93	Mn, V	-286	-1.45	Fe, Mn	9	0.05
FeMoReTi	2240	2520	0.89	Fe, Ti	-418	-1.92	Mo, Re	-2	-0.01
FeNbTaV	1840	2210	0.83	Fe, Ta	-243	-1.28	Nb, Ta	-10	-0.05
FeTaVW	2360	2360	1.00	Fe, Ta	-243	-1.19	Fe, W	-33	-0.16
HfMoReTi	2320	2370	0.98	Hf, Re	-407	-1.99	Mo, Re	-2	-0.01
HfNbReTa	620	2720	0.23	Hf, Re	-407	-1.74	Hf, Ta	49	0.21
HfNbReTi	1320	2390	0.55	Hf, Re	-407	-1.98	Hf, Nb	23	0.11
HfNbReV	1720	2430	0.71	Hf, Re	-407	-1.94	Hf, Nb	23	0.11
HfNbReW	2500	2790	0.90	Hf, Re	-407	-1.69	Hf, Nb	23	0.10
HfNbReZr	1560	2360	0.66	Hf, Re	-407	-2.00	Hf, Nb	23	0.11
HfReTaTi	1300	2480	0.52	Hf, Re	-407	-1.90	Hf, Ta	49	0.23
HfReTaV	1560	2490	0.63	Hf, Re	-407	-1.90	Hf, Ta	49	0.23
HfReTiV	1780	2220	0.80	Hf, Re	-407	-2.13	Ti, V	37	0.19
HfReTiW	1820	2530	0.72	Hf, Re	-407	-1.87	Re, W	7	0.03
HfReTiZr	1460	2160	0.68	Hf, Re	-407	-2.19	Ti, Zr	24	0.13
HfReVW	2540	2610	0.97	Hf, Re	-407	-1.81	Re, W	7	0.03
HfReWZr	1600	2650	0.60	Hf, Re	-407	-1.78	Re, W	7	0.03
IrMoNiPt	1920	2170	0.88	Mo, Pt	-366	-1.96	Ir, Pt	11	0.06
IrMoOsPd	2660	2680	0.99	Ir, Mo	-338	-1.46	Os, Pd	67	0.29
IrMoOsPt	2000	2730	0.73	Mo, Pt	-366	-1.56	Os, Pt	22	0.09
IrMoPdPt	2160	2170	1.00	Mo, Pt	-366	-1.96	Ir, Pd	40	0.21
IrMoPtRe	1080	2770	0.39	Mo, Pt	-366	-1.53	Ir, Pt	11	0.05
IrMoPtRh	1960	2370	0.83	Mo, Pt	-366	-1.79	Ir, Pt	11	0.05
IrMoPtRu	2140	2420	0.88	Mo, Pt	-366	-1.76	Ir, Pt	11	0.05
IrNbPdRh	260	2370	0.11	Ir, Nb	-830	-4.06	Ir, Pd	40	0.20
IrNiPdRe	2200	2420	0.91	Ir, Re	-274	-1.31	Ir, Pd	40	0.19
IrNiPtRe	1600	2480	0.65	Ir, Re	-274	-1.28	Ir, Pt	11	0.05
IrOsPtRe	2100	2870	0.73	Ir, Re	-274	-1.11	Os, Pt	22	0.09
IrPdPtRe	1660	2500	0.66	Ir, Re	-274	-1.27	Ir, Pd	40	0.19
IrPtReRh	1840	2610	0.70	Ir, Re	-274	-1.22	Ir, Pt	11	0.05
IrPtReRu	1920	2690	0.71	Ir, Re	-274	-1.18	Ir, Pt	11	0.05
MnMoNbRe	2180	2240	0.97	Nb, Re	-202	-1.05	Mo, Re	-2	-0.01
MnMoReV	1580	2200	0.72	Mn, V	-286	-1.51	Mo, Re	-2	-0.01
MnMoVW	2500	2560	0.98	Mn, V	-286	-1.30	Mo, W	-8	-0.04
MnNiPdRu	820	1910	0.43	Mn, Pd	-251	-1.53	Pd, Ru	47	0.29
MnOsPdRu	1080	2310	0.47	Mn, Pd	-251	-1.26	Os, Pd	67	0.34

MnReVW	1600	2700	0.59	Mn, V	-286	-1.23	Re, W	7	0.03
MoNbNiV	1740	2100	0.83	Nb, Ni	-316	-1.75	Nb, V	-56	-0.31
MoNiOsPt	1280	2190	0.58	Mo, Pt	-366	-1.94	Ni, Os	32	0.17
MoNiPdPt	1260	1920	0.66	Mo, Pt	-366	-2.21	Ni, Pd	-6	-0.04
MoNiPtRe	1440	2250	0.64	Mo, Pt	-366	-1.89	Mo, Re	-2	-0.01
MoNiPtRh	760	2070	0.37	Mo, Pt	-366	-2.05	Ni, Rh	2	0.01
MoNiPtRu	1320	2100	0.63	Mo, Pt	-366	-2.02	Ni, Ru	40	0.22
MoNiReV	1620	2210	0.73	Ni, V	-250	-1.31	Mo, Re	-2	-0.01
MoOsPdPt	1280	2190	0.58	Mo, Pt	-366	-1.94	Os, Pd	67	0.36
MoOsPdRh	1600	2570	0.62	Mo, Rh	-248	-1.12	Os, Pd	67	0.30
MoOsPtRe	2180	2930	0.74	Mo, Pt	-366	-1.45	Os, Pt	22	0.09
MoOsPtRh	1200	2620	0.46	Mo, Pt	-366	-1.62	Os, Pt	22	0.10
MoOsPtRu	1840	2710	0.68	Mo, Pt	-366	-1.57	Os, Pt	22	0.09
MoPdPtRe	1000	2290	0.44	Mo, Pt	-366	-1.85	Mo, Re	-2	-0.01
MoPdPtRh	1540	2120	0.73	Mo, Pt	-366	-2.00	Pd, Rh	37	0.20
MoPdPtRu	1360	2130	0.64	Mo, Pt	-366	-1.99	Pd, Ru	47	0.26
MoPdReRh	1820	2310	0.79	Mo, Rh	-248	-1.25	Pd, Rh	37	0.19
MoPdRhRu	2100	2130	0.99	Mo, Rh	-248	-1.35	Pd, Ru	47	0.26
MoPtReRh	780	2550	0.31	Mo, Pt	-366	-1.67	Mo, Re	-2	-0.01
MoPtReRu	580	2580	0.22	Mo, Pt	-366	-1.65	Mo, Re	-2	-0.01
MoPtRhRu	2100	2320	0.91	Mo, Pt	-366	-1.83	Rh, Ru	-8	-0.04
MoReTiZr	1820	2150	0.85	Re, Zr	-358	-1.93	Ti, Zr	24	0.13
MoReWZr	2280	2660	0.86	Re, Zr	-358	-1.56	Re, W	7	0.03
NbPdPtRh	220	2210	0.10	Nb, Pt	-721	-3.79	Pd, Rh	37	0.19
NbReTaTi	880	2590	0.34	Re, Ta	-226	-1.01	Ta, Ti	31	0.14
NbReTaZr	1440	2450	0.59	Re, Zr	-358	-1.70	Ta, Zr	36	0.17
NbReTiV	1040	2320	0.45	Nb, Re	-202	-1.01	Ti, V	37	0.19
NbReTiZr	1040	2160	0.48	Re, Zr	-358	-1.92	Ti, Zr	24	0.13
NbReVZr	2180	2190	1.00	Re, Zr	-358	-1.90	V, Zr	26	0.14
NbReWZr	2000	2640	0.76	Re, Zr	-358	-1.57	Nb, Zr	21	0.09
NiOsPtRe	1040	2640	0.39	Pt, Re	-232	-1.02	Ni, Os	32	0.14
NiPdPtRe	1160	1930	0.60	Pt, Re	-232	-1.40	Ni, Pd	-6	-0.04
NiPdReRh	1460	1990	0.73	Re, Rh	-181	-1.06	Pd, Rh	37	0.22
NiPtReRh	1380	2200	0.63	Pt, Re	-232	-1.22	Ni, Rh	2	0.01
NiPtReRu	1340	2240	0.60	Pt, Re	-232	-1.20	Ni, Ru	40	0.21
OsPdPtRe	1460	2660	0.55	Pt, Re	-232	-1.01	Os, Pd	67	0.29
PdPtReRh	1680	2240	0.75	Pt, Re	-232	-1.20	Pd, Rh	37	0.19
PdPtReRu	1560	2270	0.69	Pt, Re	-232	-1.19	Pd, Ru	47	0.24
PtReRhRu	1680	2570	0.65	Pt, Re	-232	-1.05	Rh, Ru	-8	-0.04
ReTaTiV	1080	2440	0.44	Re, Ta	-226	-1.07	Ti, V	37	0.18
ReTaTiZr	1460	2260	0.65	Re, Zr	-358	-1.84	Ta, Zr	36	0.18

ReTaVZr	2240	2270	0.99	Re, Zr	-358	-1.83	Ta, Zr	36	0.18
ReTiWZr	1820	2420	0.75	Re, Zr	-358	-1.72	Ti, Zr	24	0.12
ReVWZr	2460	2490	0.99	Re, Zr	-358	-1.67	V, Zr	26	0.12